Distribution Agreement

In presenting this thesis as a partial fulfillment of the requirements for a degree from Emory University, I hereby grant to Emory University and its agents the non-exclusive license to archive, make accessible, and display my thesis in whole or in part in all forms of media, now or hereafter now, including display on the World Wide Web. I understand that I may select some access restrictions as part of the online submission of this thesis. I retain all ownership rights to the copyright of the thesis. I also retain the right to use in future works (such as articles or books) all or part of this thesis.

Mary Rose Branch April 15, 2015

Shedding light on the spatiotemporal regulation of RGS14

by

Mary Rose Branch

Dr. John Hepler
Adviser

Neuroscience and Behavioral Biology

Dr. John Hepler

Adviser

Dr. Gary Bassell

Committee Member

Dr. Kristen Frenzel

Committee Member

Dr. Jose Soria

Committee Member

2015

Shedding light on the spatiotemporal regulation of RGS14

By

Mary Rose Branch

Dr. John Hepler

Adviser

An abstract of
a thesis submitted to the Faculty of Emory College of Arts and Sciences
of Emory University in partial fulfillment
of the requirements of the degree of
Bachelor of Sciences with Honors

Neuroscience and Behavioral Biology

2015

Abstract

Shedding light on the spatiotemporal regulation of RGS14

Mary Rose Branch

RGS14 is a multifunctional scaffold protein that integrates various cellular pathways and interacts with active (GTP-bound) and inactive (GDP-bound) Gα subunits to negatively regulate G protein signaling. RGS14 is enriched in area CA2 of the hippocampus where it acts as a natural suppressor of long-term potentiation. The functional role of RGS14 in CA2 neurons and the mechanisms by which it limits synaptic plasticity, however, are unknown. The subcellular localization of proteins in their native cellular environment can provide critical insight into their *in vivo* functions. All previous information about the subcellular localization of RGS14 relied largely on exogenous expression of recombinant protein in non-host cells. Since mislocalization of exogenously expressed proteins is a common problem that can give a false impression of the endogenous protein's distribution and *in vivo* functionalities, the primary aim of this study was to investigate the subcellular localization of endogenous RGS14 in its native cellular environment under basal conditions and following G protein activation. Because CA2 neurons cannot be isolated for study, we studied RGS14 localization in B35 neuroblastoma cells, the only cell line known to natively express RGS14. Using immunocytochemistry and confocal imaging, we found that endogenous RGS14 localizes to multiple cellular compartments in host B35 cells and that both inactive and activated G proteins can regulate the spatiotemporal dynamics of RGS14. Our results suggest that RGS14 may have multiple and complex functions in CA2 neurons, highlighting the need for future studies to determine which of these functions is critical for RGS14-mediated suppression of synaptic plasticity.

Shedding light on the spatiotemporal regulation of RGS14

By

Mary Rose Branch

Dr. John Hepler

Adviser

A thesis submitted to the Faculty of Emory College of Arts and Sciences
of Emory University in partial fulfillment
of the requirements of the degree of
Bachelor of Arts OR Bachelor of Sciences with (do not enter level of honors)Honors

Neuroscience and Behavioral Biology

2015

Acknowledgements

I would like to thank Nicole Brown, Paul Evans, Kyle Gerber, and Suneela Ramsey for mentoring, encouraging, and welcoming me into the Hepler lab— in addition, Nicole Brown for guiding and inspiring the second aim of this project; Paul Evans for advising me and teaching me good sterile technique; Kyle Gerber for his suggestions and help optimizing immunofluorescence protocols; Suneela Ramsey for her help ordering supplies. The privilege of working in the Hepler lab has been one of the most rewarding educational experiences of my undergraduate career.
I would also like to thank Dr. Maureen Powers for kindly supplying the anti-414 antibody; Dr. Richard Kahn, Laura Newman, and other members of the Kahn lab for their generosity in providing various antibodies and cell lines used in these studies. I would also like to thank Laura Newman for her invaluable advice and guidance in troubleshooting immunofluorescence protocols and confocal imaging. I would like to extend my deep gratitude to my committee members, Dr. Gary Bassell, Dr. Kristen Frenzel, and Dr. Jose Soria—their support, input, and advice have been invaluable throughout the duration of my project. Finally, I would like to extend a special thanks to my thesis advisor, Dr. John Hepler. Without his continued guidance, support, occasional pushing, and funding, this project would not have been possible.

This work was funded in part by the Scholarly Research at Emory (SIRE) program.

Table of Contents

Illustrations

Figures

Tables

BACKGROUND AND SIGNIFICANCE

Long-term potentiation (LTP), a long-lasting increasing in synaptic strength following brief periods of stimulation, is often considered the molecular correlate of learning and memory and is one of the major hallmarks of the hippocampus. The hippocampus, a region of the brain within the limbic system, has a critical role in the formation of new episodic, social, and spatial memories. The flow of excitatory neurotransmission within the hippocampus has traditionally focused on the (DG)-CA3-CA1 "tri-synaptic" circuit as integral to hippocampal-based learning and memory (Neves et al., 2008); nevertheless, relatively little is known about neighboring area CA2—which was previously considered to be an inactive transition zone. CA2 pyramdial neurons are anatomically and physiologically distinct from pyramidal neurons within areas CA1 and CA3 in that they are also protected from ischemic and seizure-induced damage and naturally resistant to LTP (Kirino, 1982; Sloviter, 1991; Zhao et al., 2007). Growing evidence suggests that area CA2 is important for social behavior and is impaired in individuals with bipolar disorder and schizophrenia (Benes et al., 1998; Caruana et al., 2012; Hitti and Siegelbaum, 2014; Pagani et al., 2014; Stevenson and Caldwell, 2014); nevertheless, the mechanisms regulating neuroprotection and synaptic plasticity in area CA2 are poorly understood because CA2 neurons exhibit a unique gene and protein expression pattern that differs from those of its neighboring CA regions (Lein et al., 2005).

One such protein predominantly expressed in area CA2 is a multifunctional regulator of G protein signaling known as RGS14 (Lee et al., 2010). Regulator of G protein signaling (RGS) proteins constitute an architecturally and functionally diverse family of nearly 40 members that share a common ~ 120 amino acid binding domain that interacts with activated (GTP-bound) Gα subunits. RGS proteins negatively regulate G protein signaling by acting as GTPase accelerating

proteins (GAPs) to stimulate the intrinsic GTP hydrolysis of their interacting Gα binding partners (reviewed in Watson et al., 1996; Hollinger and Hepler, 2002). In addition to the conserved RGS domain that acts as a GAP for $G\alpha_{i/o}$-GTP subunits, RGS14 contains a G protein regulatory (GPR/GoLoco) motif that binds inactive $G\alpha_i$-GDP subunits and tandem Ras/Raf binding domains (RBDs) (Cho et al. 2000; Traver et al., 2000; Hollinger et al., 2001; Kimple et al., 2001; Mittal and Linder, 2004). The presence of its two Gα binding domains, the GPR motif and conserved RGS domain, allows RGS14 to bind both active and inactive Gα subunits and potentially regulate multiple G protein signaling pathways at one time. Indeed, previous studies have shown that RGS14 can engage both conventional (GPCR-activated) and unconventional G protein signaling events (reviewed in McCudden et al., 2005).

Our lab has recently reported that mice lacking RGS14 (RGS14-KO) exhibit robust LTP at Schaffer collateral (SC)-CA2 synapses, accompanied by enhanced spatial learning and object recognition compared to their wild type littermates. Notably, RGS14-KO mice do not differ in LTP in CA1 neurons, indicating that LTP in area CA2 contributes to the enhanced learning/memory seen in the RGS14-KO mice (Lee et al., 2010). In addition, adenovirus (AAV)-mediated expression of RGS14 in CA1 hippocampal neurons suppresses LTP (unpublished data), suggesting that RGS14 inhibits cellular pathways underlying LTP induction that are common to both CA2 and CA1 neurons; the mechanism(s) by which RGS14 inhibits LTP, however, is unknown.

RATIONALE

At the cellular level, our lab hypothesizes that the subcellular localization of RGS14 expression may change to serve multiple roles in different cellular compartments, depending on the state of the cell. Considerable evidence supports this idea; native RGS14 exists in both

cytosolic and membrane fractions of rat brain extracts (Hollinger et al., 2001) and is visible within the soma, dendrites, spines, and post-synaptic terminals of CA2 pyramidal neurons by electron microscopy (Lee et al., 2010; Evans et al., 2014). Furthermore, previous immunofluorescent imaging studies have shown that exogenous RGS14 localizes to centrosomes and shuttles between the nucleus and cytoplasm when expressed in HeLa cells and is recruited to the plasma membrane following expression of inactive $G\alpha_{i1}$-GDP or activated H-Ras-GTP (Cho et al., 2005; Cho et al., 2007; Shu et al., 2007; Vellano et al., 2013). Taken together, these findings suggest that RGS14 is dynamically regulated and serves multiple functions depending on its subcellular localization and state of the cell.

One limitation of these previous cell-based studies, however, is that they have all relied on exogenously expressed epitope tagged-RGS14 in cells that do not naturally express RGS14 at detectable protein levels. To date, very little is known about native RGS14 in its host cellular environment. *Understanding the spatiotemporal dynamics of proteins within host cells can provide vital insight into their native cellular functions*. Nevertheless, most of what we know about RGS14 in cells is based on the behavior of ectopically expressed recombinant RGS14 in non-native cells. Whether this reflects the behavior of native RGS14 in its natural environment is unknown. In addition to CA2 pyramidal neurons, B35 cells—derived from rat neuroblastoma—are the only mammalian cell line we have found to express detectable levels of RGS14 protein by immunoblot (**Fig. 2**).

Hypotheses and Aims

Based on its architecturally complex multi-domain structure and studies with exogenously expressed recombinant protein, we *hypothesized* that 1) native RGS14 localizes to multiple cellular compartments in host cells and 2) G protein activation can modulate the

spatiotemporal targeting of RGS14 from various basal state subcellular compartments to the plasma membrane. Therefore, the *goal* of these studies was two fold: 1) identify the subcellular localization of endogenous RGS14 in its host cellular environment and 2) determine the extent to which the activation of G proteins affects its cellular distribution.

Since the localization and function of RGS14 in its non-native environment may not accurately reflect the role of RGS14 in natural host neuronal cells (Stadler et al., 2013), *the first aim of this project was to identify the dynamic localization of native RGS14 under different conditions in cells from a neuronal lineage that naturally express detectable levels of RGS14*. In addition, although there is much evidence to suggest that the subcellular localization of exogenous RGS14 is regulated by its interactions with inactive $G\alpha_{i1/3}$ via the GPR motif, unknown is whether interactions with activated Gα subunits through the RGS domain also influence the cellular distribution of RGS14. Therefore, *the second goal of this project was to explore whether activated Gα binding partners affect the subcellular localization of RGS14*. We hypothesized that if both the RGS domain also serves to regulate the functional localization of RGS14, then G protein activation would lead to a redistribution of RGS14 from basal state cellular compartments.

Electron micrographs of CA2 neurons from fixed hippocampal slices revealed that endogenous RGS14 is visible in various microdomains in host CA2 pyramidal neurons (Lee et al., 2010); *we, therefore predicted that endogenous RGS14 also exists in multiple subpopulations within B35 cells*. Furthermore, since other RGS proteins have been shown to translocate to the plasma membrane in response to GPCR agonist- and AlF_4^- -induced G protein activation (Dulin et al., 1999; Cho et al., 2003; Roy et al., 2003), *we predicted that application of AlF_4^- would also affect the subcellular localization of RGS14*.

MATERIAL AND METHODS

Cell Culture and Transfection

Rat neuroblastoma (B35), Human cervical carcinoma (HeLa), African Green Monkey kidney (Cos7), human glioblastoma (SF295), and human embryonic kidney (HEK293) cells were maintained in 1X Dulbecco's modified eagle medium with phenol red indicator (Mediatech) supplemented with 10% fetal bovine serum (Atlanta Biologicals, 5% after transfection), 100 U/mL penicillin (Mediatech), and 100 mg/mL streptomycin (Mediatech) in a humidified environment at 37°C with 5% CO_2. All transient transfections were performed using previously described methods with polyethyleneimine (PEI; Polysciences, Inc.) (Oner et al., 2010). For all experiments, the total amount of plasmid DNA used for cotransfection experiments of FLAG-RGS14 and $G\alpha_{i/o}$-EE in HeLa cells was normalized with vector DNA (pcDNA3.1) to 200 ng.

G protein Activation with AlF_4^-

For aluminum Tetrafluoride (AlF_4^-) - induced G protein activation, B35 cells were incubated with Tyrode's solution (140 mM NaCl, 5 mM KCl, 1 mM $MgCl_2$, 1 mM $CaCl_2$, 0.37 mM NaH_2PO_4, 24 mM $NaHCO_3$, 10 mM HEPES, and 0.1% glucose, pH 7.4) supplemented with or without (control) 10 mM NaF, 9 mM $MgCl_2$, and 30 μM $AlCl_3$ for indicated times at 37 °C. AlF_4^- -induced activation experiments with HeLa cells were performed for 10 min at room temperature.

Immunofluorescence

In this study, we extensively compared four different fixation and permeabilization methods (detailed in the flow chart in **Figure 1**) to determine the distribution of native RGS14 in B35 cells. Unless otherwise stated, native RGS14 was visualized using the methanol fixation protocol (Figure 1), followed by immunostaining with an anti-RGS14 polyclonal primary antibody (RGS14 pAb; 1:400) and Alexa594 secondary antibody. Briefly, B35 cells were fixed in 100% ice-cold methanol for 5 min at -20 °C, rinsed twice in 1X phosphate buffered saline (PBS), and once in PBS-Tween (0.05% Tween in 1X PBS). After rinsing, cells were blocked in PBS containing 8% BSA for 1 hour at room temperature, and incubated with primary antibody in PBS containing 4% BSA (antibody buffer) overnight at 4 °C. B35 cells were then washed for 5 min PBS-Tween 3 times, incubated with Alexa 594 goat anti-rabbit and/or Alexa 488 goat anti-mouse secondary antibody (1:1000; Molecular Probes) in antibody buffer for 1-1.5 hours at room temperature, rinsed once in PBS-Tween, and washed twice for 5 min each in 1X PBS, stained with cell viable Hoechst 33342 DNA dye (1:5000) in antibody buffer for 4 min, washed again in 1X PBS, and mounted onto slides with ProLong Diamond Antifade mounting media (Invitrogen). **Table 1** shows a comprehensive list of the antibodies and corresponding concentrations used in both immunofluorescence and immunoblotting protocols.

For pre-adsorption assays, anti-RGS14 pAb or mAb (at a concentration of 1:400 or 1:300, respectively) was incubated with 1.28 ng/µl of purified recombinant rat RGS14 (kindly provided by Nicole Brown) on a rotator overnight at 4 °C prior to immunostaining. Pre-adsorption assays were performed with B35 cells fixed and permeabilized with methanol or 4% PFA and 0.1% Triton-X.

To compare the cellular distribution of FLAG-RGS14 in different cell types, B35, HeLa, Cos7, SF295, and HEK293 cells were transiently transfected with 100-500 ng of FLAG-RGS14 as previously described (PEI; Polysciences, Inc.) (Oner et al., 2010). Twenty-four hours after transfection, cells were fixed with 4% PFA and permeabilized with 0.1% Triton-X in PBS for 10 minutes each and processed for immunofluorescence as described in Brown et al. (2015).

Experiments investigating the translocation of FLAG-RGS14 in the presence of inactive or AlF_4^- -activated $G\alpha_{i/o}$ were performed as described in Brown et al. (2015). Briefly, HeLa cells were transiently transfected with 100 ng of FLAG-RGS14 and/or 100 ng of glutamate-glutamate (EE) tagged Gα subunits ($G\alpha_{i1}$-EE or $G\alpha_o$-EE). G protein activation with AlF_4^- was carried out at room temperature for 10 min. HeLa cells were rinsed in 1X PBS, fixed with 4% paraformaldehyde (PFA), permeabilized with 0.1% Triton-X in PBS for 10 min each, and immunostained as described (Brown et al., 2015).

Microscopy

Phase contrast images of B35 cells were taken using a 40X objective on an Olympus IX51 inverted fluorescence microscope (Olympus) under phase contrast settings. Confocal imaging was performed using a 60X oil immersion objective on Olympus FV1000. Fluorescence channels were scanned sequentially and averaged to avoid bleed through. Images were processed and intensity graphs generated using ImageJ software (NIH).

Immunoblotting

Mouse brain lysates were kindly provided by Paul Evans (Hepler lab, Emory University) and prepared as in Evans et al. (2014). Immunoblotting experiments were carried out as descried in Evans et al (2014) with a few modifications. Briefly, B35 cells were lysed on ice in buffer

containing 50 mM Tris-HCl, pH 8.0, 150 mM NaCl, 1 mM EGTA, 1 mM EDTA, 2 mM dithiothreitol, 10 mM MgCl2, protease inhibitor cocktail (Roche), and 1% TritonX-100. Cell lyastes were incubated on a rotator for 1 hour at 4°C, and then cleared by centrifugation at 100,000 × g for 30 min at 4°C. Lyastes were mixed with Laemmli sample buffer and boiled for 5 min. Samples from the cell lysates and mouse brain homogenates were loaded onto 11% acrylamide gels, resolved by SDS-PAGE, transferred to nitrocellulose membranes. After blocking nitrocellulose membranes for 1 hour at room temperature in blocking buffer containing 5% nonfat milk (w/v), 0.1% Tween-20, and 0.02% sodium azide, diluted in 20 mM Tris buffered saline, pH 7.6, membranes were incubated with primary antibodies diluted in the same buffer overnight at 4°C or for 2 hours at room temperature. Membranes were then washed in Tris buffered saline containing 0.1% Tween-20 (TBST) and incubated with either an anti-mouse (1:5000) or anti-rabbit (1:25,000) HRP-conjugated secondary antibody diluted in TBST for 1.5 hours at room temperature. Protein bands were detected by enhanced chemiluminescence.

Analysis of Translocation

Translocation of endogenous RGS14 in response to AlF_4^--induced G protein activation was assessed by immunofluorescence and confocal microscopy. After staining B35 cells treated with AlF_4^- for 10 min (n = 35) or left untreated (control; n= 35) with anti-RGS14 pAb to detect endogenous RGS14, the fluorescence intensity around the nuclear membrane was compared to the fluorescence intensity within the cytoplasm using ImageJ software. Hoechst DNA stain, visualized under the DAPI channel on the confocal microscope, was used to locate the nucleus and the area around the nuclear membrane was traced with the freehand tracing tool in ImageJ. Translocation was considered a significant difference in relative fluorescence staining around the nuclear membrane between untreated (control) and AlF_4^-- treated cells. Relative nuclear

membrane fluorescence was determined by dividing the mean fluorescence intensity around the nuclear membrane by the mean fluorescence intensity in a comparable sized area within the cytosol (**Supplementary Fig. 1**). All non-dividing cells from randomly selected fields pooled from 3 independent experiments were included in the analysis.

Statistical Analysis

Statistical analysis was carried out using GraphPad Prism software. Comparisons between control and AlF_4^- -treated B35 cells (n = 35 cells per group) were performed using a two-tailed unpaired t-test with $P < 0.05$ considered statistically significant. Data are reported as mean +/- s.d.

Statement of authenticity

Unless otherwise noted, all experiments performed for this thesis were conducted by the author, Mary Rose Branch.

Table 1: List of antibodies used in this study

Primary antibody	Host	Concentration	Secondary antibody *	Provider
RGS14 mAb	mouse	1:300 (ICC); 1:300 (IB)	Alexa 488 goat anti-mouse; anti-mouse (1:500) for IB	NeuroMab
RGS14 pAb	rabbit	1:400 (ICC); 1:250 (IB)	Alexa 594 goat anti-rabbit; anti-rabbit (1:25,000) for IB	Proteintech
FLAG	rabbit	1:1000 (ICC)	Alexa 594 goat anti-rabbit	Sigma
EE	mouse	1:1000 (ICC)	Alexa 488 goat anti-mouse	Covance
β-III tubulin	rabbit	1:800 (ICC)	Alexa 488 goat anti-rabbit	Sigma
414 mAb	mouse	1:8000 (ICC)	Alexa 488 goat anti-mouse	A kind gift from Dr. Maureen Powers, Emory University
KDEL receptor (KDELR) §	mouse	1:1000 (ICC)	Alexa 488 goat anti-mouse	Stressgen
GRP78/BiP §	mouse	1:200 (ICC)	Alexa 488 goat anti-mouse	Stressgen
HSP60 §	mouse	1:5000 (ICC)	Alexa 488 goat anti-mouse	Stressgen
GM130 §	mouse	1:1000 (ICC)	Alexa 488 goat anti-mouse	BD Transduction
Transferrin receptor (TfR) §	mouse	1:1000 (ICC)	Alexa 488 goat anti-mouse	Zymed
Trans Golgi network (TGN) §	mouse	1:1000 (ICC)	Alexa 488 goat anti-mouse	BD Transduction
α-tubulin §	mouse	1:1000 (ICC)	Alexa 488 goat anti-mouse	Sigma
β-tubulin §	mouse	1:1000 (ICC)	Alexa 488 goat anti-mouse	Sigma
γ-tubulin §	mouse	1:1000 (ICC)	Alexa 488 goat anti-mouse	Sigma
Mannose 6 phosphate receptor: CI/300 §	mouse	1:1000 (ICC)	Alexa 488 goat anti-mouse	Gift to the Kahn lab from Annette Hille-Rehfeld

* All Alexa secondary antibodies were used at a concentration of 1:500 or 1:1000 (B35 cells)

§ Antibodies generously provided by Dr. Richard Kahn's lab, Emory University

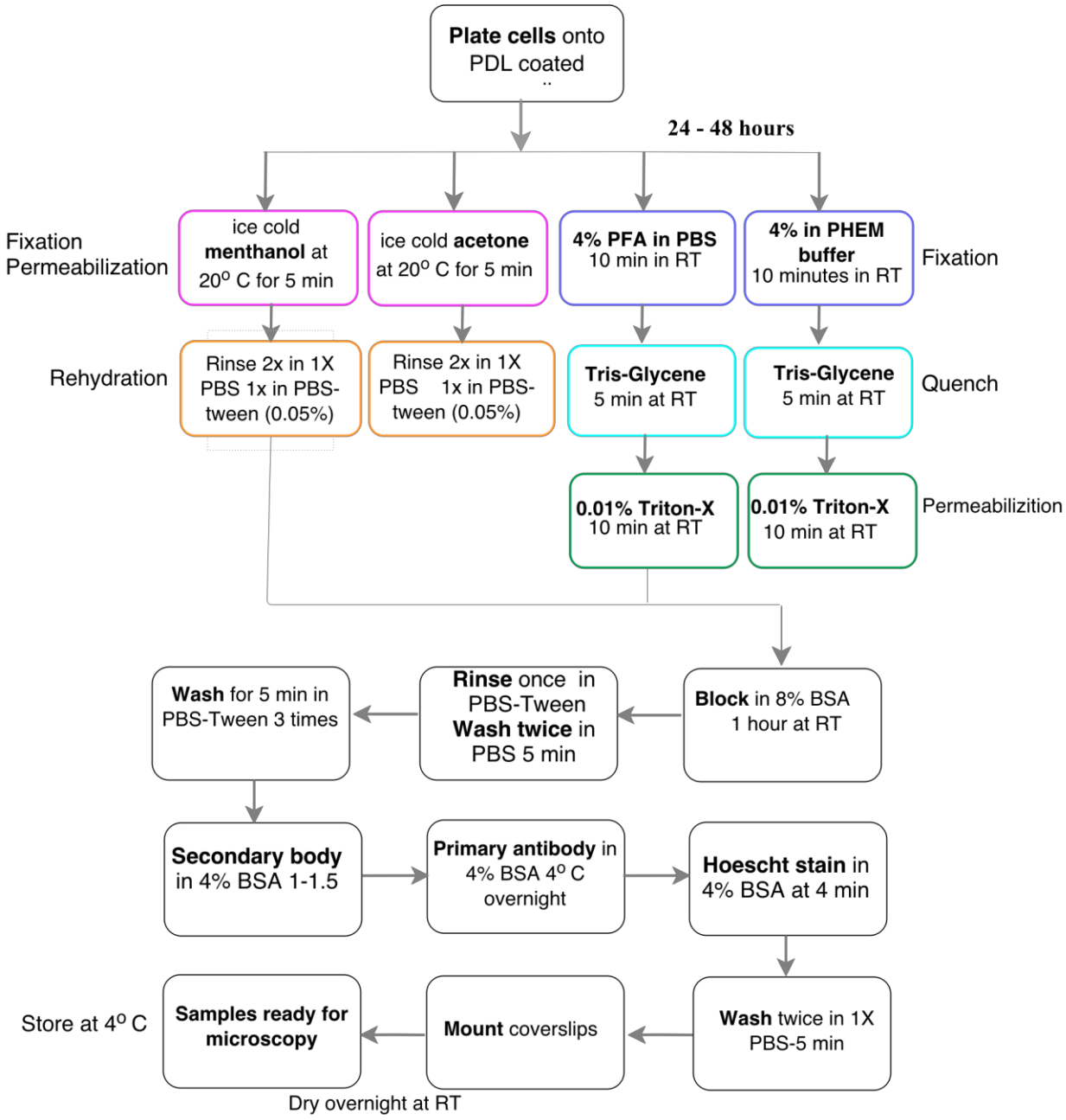

Figure 1l A flowchart diagram showing the different immunofluorescence protocols used in this study to visualize endogenous RGS14 in B35 cells. PFA; paraformaldehyde. PHEM buffer; 60 mM PIPES, 25 mM HEPES, 10 mM EGTA, 2 mM MgCl2, pH 6.9. Tris-Glycine; 200 mM Tris, 0.75% glycine, pH 7.4.

RESULTS

RGS14 is endogenously expressed in B35 cells

Immunoblotting with a previously characterized monoclonal anti-RGS14 antibody (Lee et al., 2010; Evans et al., 2014) confirmed the expression of endogenous RGS14 in both mouse brain and B35 cells (Hollinger et al., 2003; Evans et al., 2014) (**Fig. 2b**). To investigate the subcellular localization of endogenous RGS14, we compared several immunofluorescence protocols (**Fig. 1**) with two different anti-RGS14 antibodies. Although the specific monoclonal antibody (RGS14 mAb) detected RGS14 as a single band at the appropriate molecular weight (61 kD) in mouse brain and B35 cells (**Fig. 2b**), it showed a weak staining pattern with immunofluorescence (**Fig. 3**) that was undetectable when visualized under a standard fluorescence microscope (data not shown). High-resolution confocal imaging revealed that when B35 cells were fixed with paraformaldehyde and permeabilized with Triton X-100, the RGS14 mAb showed a diffuse staining pattern equally distributed throughout the cytosol and nucleus. The RGS14 mAb showed considerably less cytosolic staining, but intense punctate staining within the nucleus after fixing with organic solvents (methanol or acetone). The decrease in apparent cytoplasmic staining may be due to some amount of cytosolic protein extraction known to occur with fixation using organic solvents (Schnell et al., 2012). The absence of pronounced immunofluorescence staining in B35 cells with paraformaldehyde fixation using the RGS14 mAb, despite evident detection of RGS14 by immunoblot (**Fig. 2b, 3a**), may be due to steric hindrance or loss of antigenicity caused by protein or epitope cross-linking (respectively) during fixation (Lipman et al., 2005; Schnell et al., 2012).

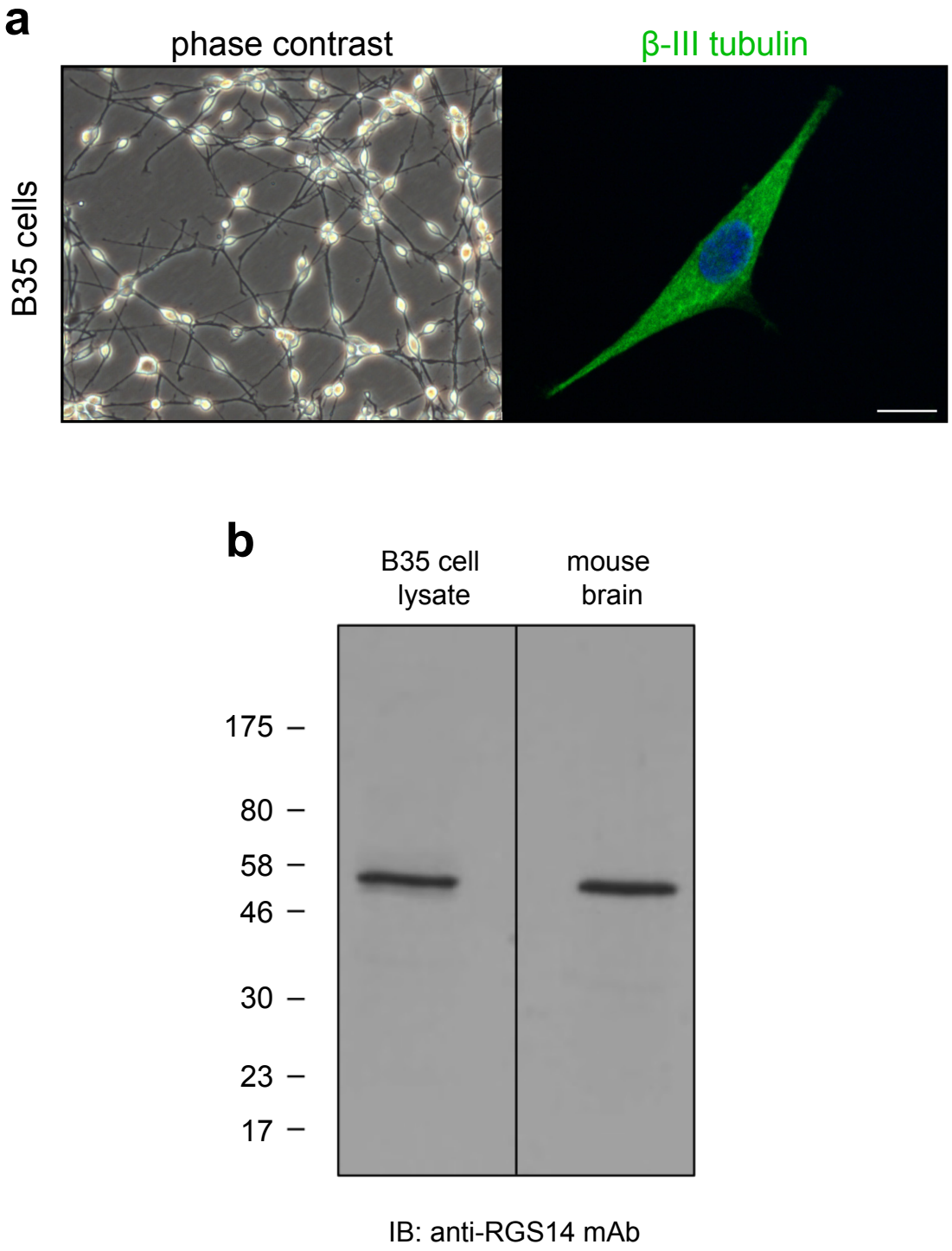

Figure 2 | RGS14 is natively expressed in mouse brain and B35 cells. (a) B35 cells are a rat neuroblastoma cell line that have neuron-like processes and express neuron specific β-III tubulin. Phase contrast image of undifferentiated B35 cells highlights B35 cell neurites. Confocal image of a B35 cells immunostained with neuron-specific β-III tubulin antibody. Scale bar, 10 μm. (b) RGS14 is expressed at detectable levels by immunoblot in mouse brain and B35 cell lysates using a specific monoclonal antibody (RGS14 mAb).

Though monoclonal antibodies are useful due to their high specificity in binding to a single antigenic site on their target protein, in some cases, they can have limited use in immunofluorescence experiments as a result of weak staining and/or low signal-to-noise. Conversely, polyclonal antibodies, though often less specific than monoclonal antibodies, bind to multiple antigenic sites and, thus, tend to provide higher signal-to-noise detection with immunofluorescence analysis. Consequently, we additionally stained B35 cells with a polyclonal antibody that also detected RGS14 by immunoblot in B35 cells (**Fig. 3a**).

The RGS14 polyclonal antibody (RGS14 pAb) showed a more robust staining pattern than the RGS14 mAb for all fixation and permeabilization methods tested (**Fig 4**); however, immunofluorescence signal specificity was confirmed for both antibodies by a reduction in staining observed when the anti-RGS14 antibodies were pre-incubated (absorbed) with purified full-length recombinant RGS14 (**Fig. 3b**). Following methanol fixation, immunolabeling B35 cells with the RGS14 pAb and mAb showed endogenous RGS14 localization in the cytoplasm and in unidentified nuclear bodies (**Fig. 3b**,**c**), while exogenously expressed FLAG-RGS14 was predominantly located within the cytosol (**Fig. 4**). The RGS14 pAb, however, showed additional localization of endogenous RGS14 around the nuclear membrane, which was observed under all fixation/permeabilization protocols tested (**Fig. 4**).

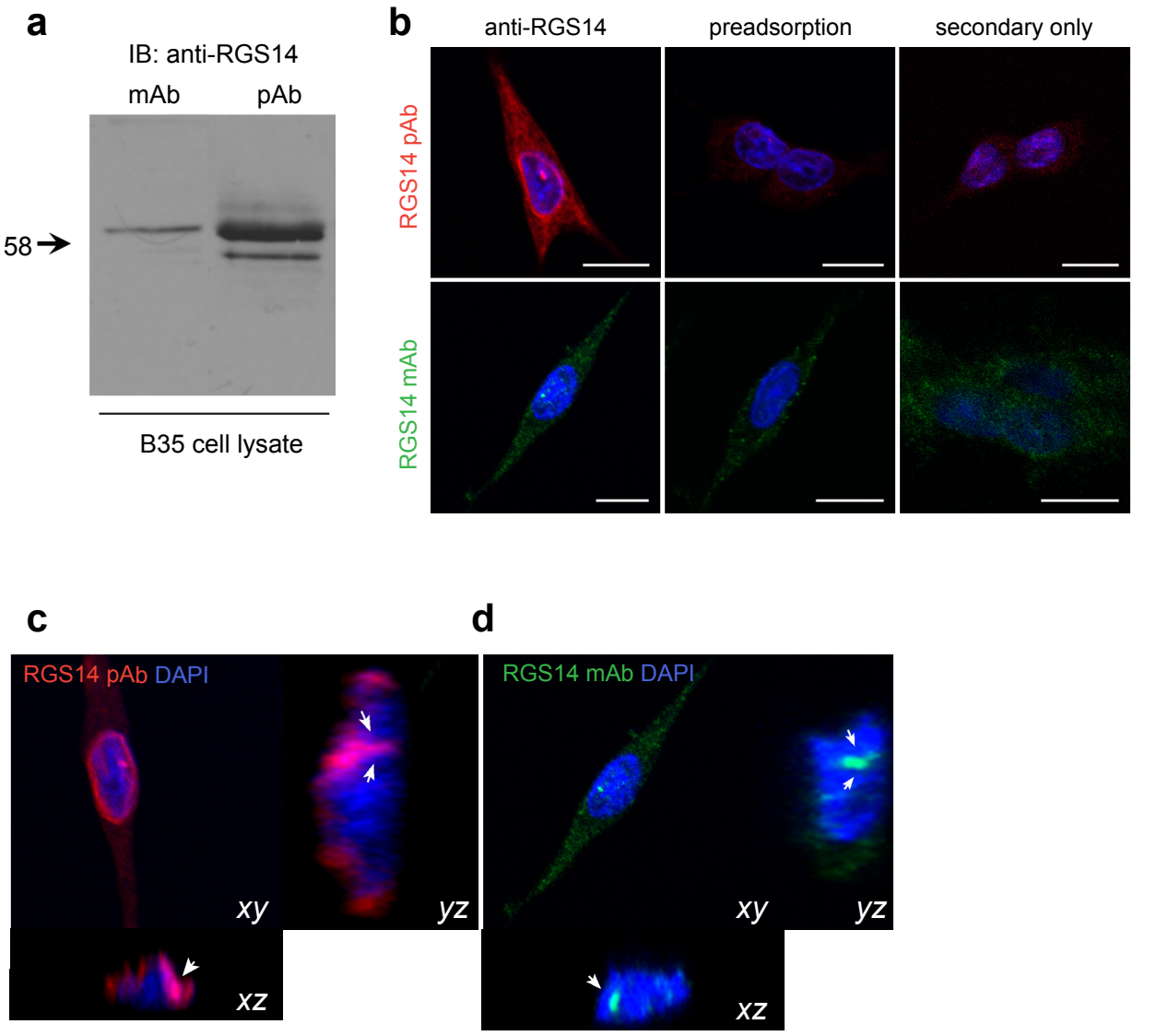

Figure 3| Immunostaining with anti-RGS14 antibodies detects endogenous RGS14 in B35 cells. (a) Endogenous RGS14 is detected by immunoblot in B35 cell lysates. RGS14 monoclonal (mAb) and polyclonal (pAb) antibodies both detect a band at ~61 kD. The RGS14 pAb showed an additional band at a slightly lower molecular weight, which could represent a splice variant, degradation product, or subpopulation of RGS14 protein with different post-translational modifications. (b) Confocal images of B35 cells immunostained with RGS14 mAb and pAb following methanol fixation. Immunostaining with the RGS14 mAb and pAb indicates that endogenous RGS14 is localized in the cytosol and nucleus in B35 cells. Though the mAb and pAb showed apparent differences in the distribution of endogenous RGS14, both antibodies showed a decrease in staining intensity when preadsorbed with purified full-length recombinant RGS14. (c) Orthogonal views of confocal z stacks taken of B35 cells stained with RGS14 mAb and pAb show endogenous RGS14 localizes to nuclear subcompartments in B35 cells. Scale bar, 10 μm.

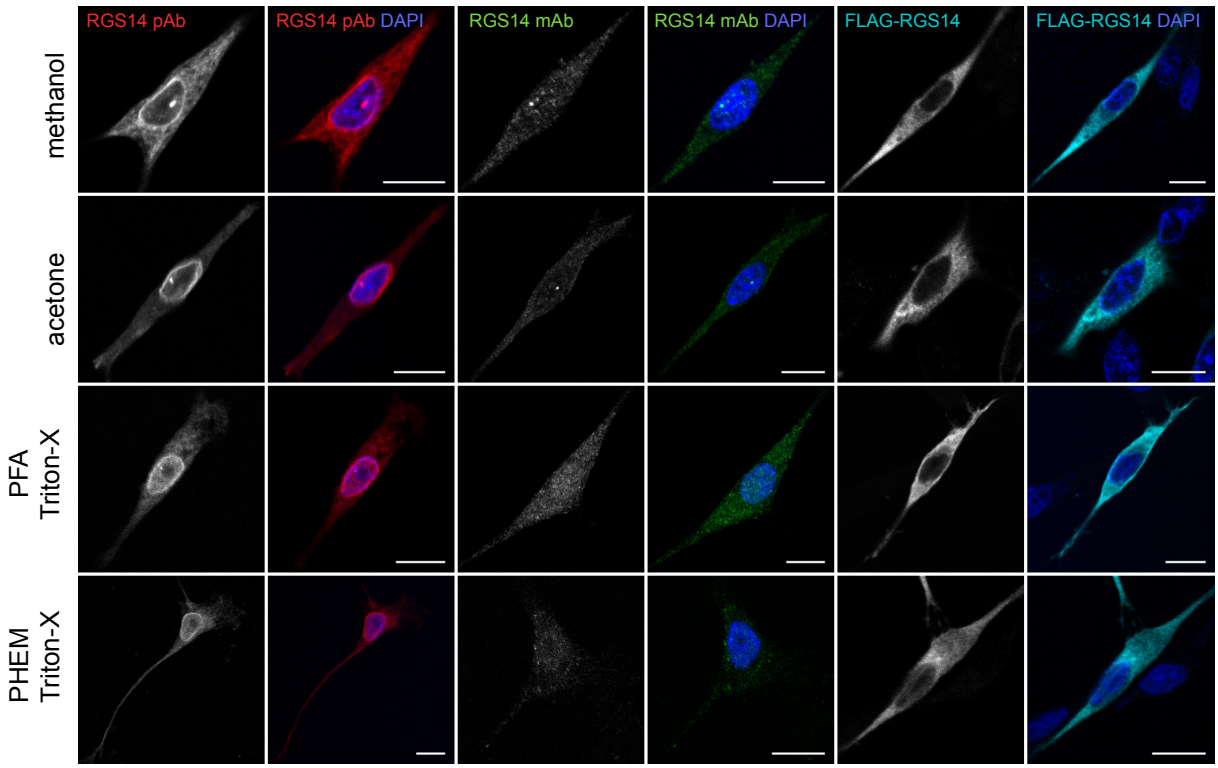

Figure 4| Localization of endogenous and exogenous RSG14 in B35 cells using different fixation and permeabilization methods. Fixation and permeabilization can affect the apparent localization and epitope accessibility of proteins (Schnell et al., 2012). Confocal images of B35 cells showing apparent distribution of endogenous RGS14 using RGS14 polyclonal (RGS14 pAb, red) and monoclonal (RGS14 mAb, green) antibodies and exogenously expressed FLAG-RGS14 detected with a FLAG antibody (cyan) after different fixation and permeabilization immunofluorescent protocols. DNA was stained by using a Hoechst stain (DAPI, blue). B35 cells were fixed and permeabilized with ice cold methanol or acetone at – 20 °C for 5 min or fixed with 4% paraformaldehyde in PBS (PFA) or PHEM buffer (PHEM) for 10 min at room temperature and subsequently permeabilized with 0.1% Triton-X (Triton) for 10 min. After blocking in PBS containing 8% BSA for 1 hour at room temperature, cells were incubated in antibody buffer (4% BSA in PBS) containing RGS14 pAb (1:400), RGS14 mAb (1:300), or FLAG (1:1000) primary antibodies overnight at 4 °C. Alexa-594 anti-rabbit secondary antibody (1:1000) was used to detected RGS14 pAb and FLAG (pseudo-colored cyan); Alexa488 anti-mouse secondary was used to detect RGS14 mAb. Scale bar, 10 μm.

Subcellular localization of endogenous RGS14 in B35 cells

To gain more insight into the intracellular distribution of endogenous RGS14, we co-stained B35 cells with the RGS14 pAb and several antibodies specific for endogenous markers (i.e.. cellular organelles and compartments). The RGS14 pAb was used in co-staining experiments because it gave a much more robust signal than the RGS14 mAb in all immunofluorescence protocols tested (**Fig. 4**). Different fixation and permeabilization conditions were also evaluated for co-staining experiments because protein components of membranous organelles and cytoskeletal structures are preserved to varying extents by different fixation and permeabilization methods. Colocalization of RGS14 with organelle markers was evaluated visually by merging the red and green fluorescent channels (**Fig. 5**). We found no significant colocalization between RGS14 and the cytoskeleton (F-actin, β-tubulin, and α-tubulin), centrosomes (γ-tubulin), endoplasmic reticulum (KDEL receptor and GRP78/BiP), trans-Golgi network (TGN38) (**Fig 7**), lysosomes (Mannose 6 phosphate receptor), or nuclear pore complexes (nuclear pore complex 414) under basal conditions in non-dividing (interphase) B35 cells. Though the RGS14 pAB showed a similar staining pattern around the nucleus as the monoclonal antibody 414 mAb used to detect nuclear pore complexes (NPCs), a merged image of the two fluorescent channels revealed only partially overlapping signals similar to those observed in cells co-stained with antibodies against NPCs and nuclear lamina (inner nuclear membrane). Although we did not co-stain with a nuclear membrane marker, the similarity in staining pattern between RGS14 pAb and mAb 414, but absence of overlapping signals, suggests that RGS14 is located around either the outer or inner nuclear membrane under basal conditions in B35 cells.

Methanol fixation can potentially lead to soluble protein extraction, while paraformaldehyde fixation cross-links soluble cytoplasmic proteins to stabile insoluble protein

structures (Schnell et al., 2012). With paraformaldehyde fixation, we observed a distribution of more intense RGS14 staining in the same regions as the inner mitochondrial matrix protein HSP60 used to label mitochondria, but only weak observable colocalization (**Fig. 5**). Notably, this colocalization was not detectable in methanol fixed B35 cells (**Supplementary Fig. 1**). It is, therefore, possible that RGS14 is localize to regions around or on the surface of mitochondria and while RGS14 association with mitochondria is preserved with paraformaldehyde fixation, surface-level localization is disrupted with methanol fixation.

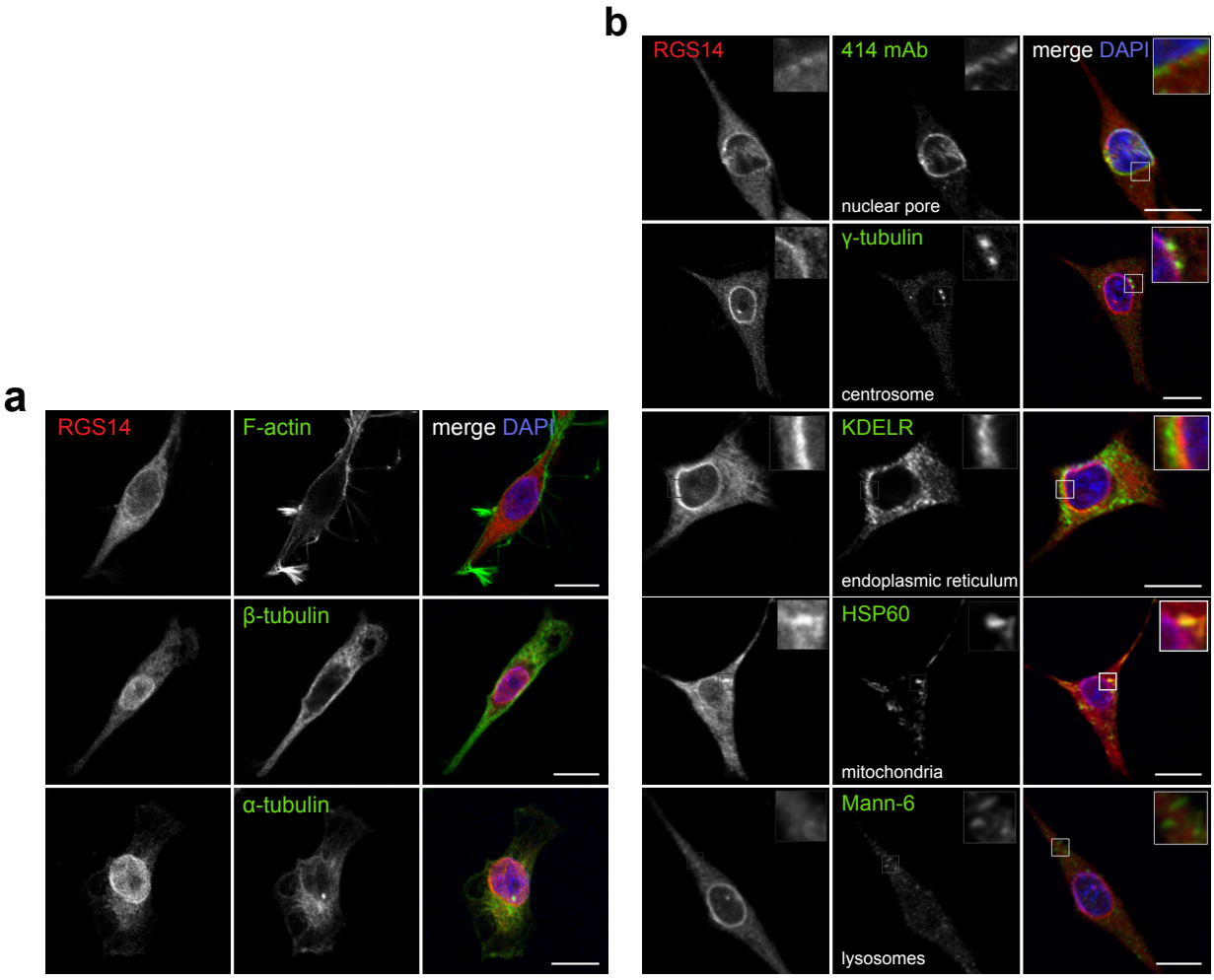
a
RGS14
F-actin
merge DAPI
β-tubulin
α-tubulin
b
RGS14
414 mAb
merge DAPI
nuclear pore
γ-tubulin
centrosome
KDELR
endoplasmic reticulum
HSP60
mitochondria
Mann-6
lysosomes
c
max intensity projection
3D rendering
z-slice
detail
nuclear pore
RGS14
414 mAb
DAPI
mitochondria
RGS14
HSP60
DAPI

Figure 5| Subcellular distribution of endogenous RGS14 in B35 cells. B35 cells were fixed and co-stained with RGS14 pAb and one of several organelle markers. B35 cells co-stained with antibodies against F-actin (**a**) and mitochondria marker HSP60 (**b**) were fixed with 4% paraformaldehyde in PBS. B35 cells co-stained with α- and β-tubulin (**a**) were fixed with 4% PFA in PHEM microtubule stabilizing buffer. B35 cells co-stained with all other organelles (nuclear pore complex, 414 mAb; γ-tubulin, centrosomes; endoplasmic reticulum, KDELR; lysosomes; Mann-6) (**b**) were fixed with methanol. Insets represent magnified boxed regions. Scale bar, 10 μm. (**c**) *Row 1* shows a representative confocal image of B35 cell with intense localization around the nuclear membrane. Maximum intensity projection and 3D reconstruction of confocal z stacks (created using ImageJ software) showing intense staining of RGS14 in a similar, but non-overlapping, pattern as nuclear pore complex marker 414 mAb as a cap around the nucleus. Magnified image (detail) highlights an area from the z slice around the nuclear membrane. *Row 2* shows a maximum intensity projection and 3D reconstruction of a confocal z stack of a B35 cell co-stained with RGS14 pAb and mitochondria marker HSP60. Magnified image (detail) highlights a region of colocalization.

The cellular distribution of RGS14 changes throughout the cell cycle

Within a given population of B35 cells that were asynchronous in their stage of the cell cycle, we observed some variation in the intensity of RGS14 staining around the nuclear membrane and within nucleus, suggesting that the localization of endogenous RGS14 in B35 cells may change as cells progress through the cell cycle. Further, we noticed that RGS14 appeared to localize to perinuclear dots in cells with less intense staining around the nuclear membrane. Though our initial investigations revealed no significant co-localization between RGS14 pAb and centrosome marker γ-tubulin in asynchronous B35 cells (**Fig. 5**), a more thorough investigation revealed that RGS14 localizes to regions near, but not directly associated with, centrosomes at certain stages of the cell cycle (**Fig. 6a**). Notably, the endogenous RGS14 signal in the vicinity of the centrosome is coincident with previously reported staining patterns of exogenous RGS14 when co-transfected with inactive $G\alpha_{i1}$ (Shu et al., 2007). In addition, though our observations came from an asynchronous cell population, we noticed that perinuclear RGS14 staining was primarily found in cells with single (unduplicated) centrosomes— presumably in phase G1. In contrast, we detected no prominent perinuclear RGS14 staining in cells with

centrosomes presenting as a doublet (late S/early G2), but instead observed an increase in RGS14 localization within nuclear subcompartments (**Fig 6a**).

RGS14 localized to the midzone during anaphase/telophase and colocalized with α-tubulin at the midbody during cytokinesis (**Fig. 6b**). It is important to note that the cell cycle stages reported here are based on visual appearance of the nucleus and centrosomes labeled with γ-tubulin of cells from an asynchronous cell population; further cell cycle arrest analysis of synchronous cell population will be necessary to confirm these observations. Nevertheless, these findings provide evidence that the distribution of endogenous RGS14 in undifferentiated B35 cells is cell cycle-dependent and support a role for RGS14 in regulating cell division.

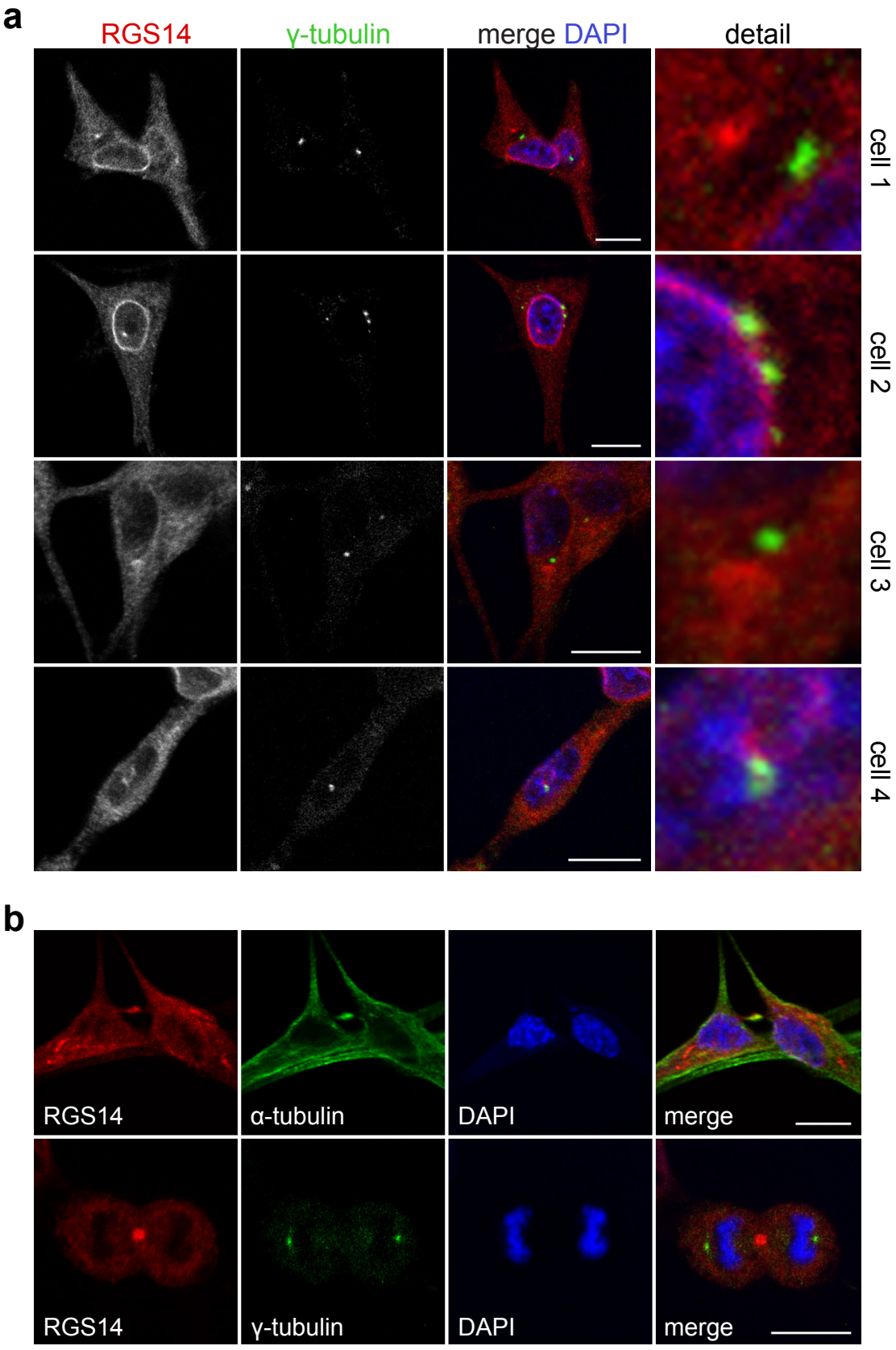
a
RGS14
γ-tubulin
merge DAPI
detail
cell 1
cell 2
cell 3
cell 4
b
RGS14
α-tubulin
DAPI
merge
RGS14
γ-tubulin
DAPI
merge

Figure 6| Distribution of endogenous RGS14 is cell cycle-dependent in B35 cells. (**a**) Confocal images B35 cells co-stained with RGS14 polyclonal antibody (pAb), centrosome marker γ-tubulin, and Hoescht stain (visualized under the DAPI channel) shows that RGS14 localizes to perinuclear regions in the vicinity of centrosomes (sites of microtubule nucleation initiation). The proximity of RGS14 to centrosomes appears to be cell cycle-dependent. Intense perinuclear staining is more apparent in cells with a single, unduplicated centrosome (*rows 1*,*3*, and *4*) non-existent in cells with centrosomes appearing as a duplicated pair (*row 2*). (**b**) RGS14 colocalizes with α-tubulin at the midbody during cytokinesis (*row 1*) and is concentrated at the midbody during anaphase/telophase (*row 2*). Scale bar, 10 μm.

AlF_4^- -induced G protein activation affects the subcellular localization of endogenous RGS14 in B35 cells.

We next sought to determine whether activation of endogenous G proteins with aluminum tetrafluoride (AlF_4^-), which activates G proteins by mimicking the transition state of GTP hydrolysis (Berman et al., 1996; Sprang, 1997), affected the subcellular localization of endogenous RGS14 around the nuclear membrane. Though G protein activation with AlF_4^- has been shown to recruit other RGS proteins to the plasma membrane from basal cellular compartment (Dulin et al., 1999; Roy et al., 2003), these previous studies primarily focused on less complex RGS proteins that lack a G protein regulatory (GPR) motif. GPR motifs interact with inactive Gα-GDP subunits to prevent re-assembly of the inactive heterotrimeric G protein (Gαβγ) after inaction of Gα-GTP. The GPR motif on RGS14, which specifically binds to inactive $G\alpha_{i1}$-GDP and $G\alpha_{i3}$-GDP, is thought to be a key regulator of RGS14 cellular distribution in cells (Cho et al., 2005; Shu et al., 2007). Whether the RGS domain also plays a role in directing the cellular distribution of RGS14, however, was previously unknown. We hypothesized that if the RGS domain also plays a role in regulating the subcellular localization of RGS14, then RGS14 would translocate to the plasma membrane following G protein activation with AlF_4^-.

We first examined whether activation of endogenous G proteins with AlF_4^- affected the localization of native RGS14 around the nuclear membrane in B35 cells. B35 cells were treated

with AlF_4^- for various times, fixed with paraformaldehyde or methanol, and processed for immunofluorescence using the RGS14 pAb to detect endogenous RGS14. Methanol fixation is often used to visualize proteins bound to structural cytoskeletal elements and stabilized organelles, but can lead to extraction of soluble cytosolic proteins and mobile cellular compartments. Since fixation with paraformaldehyde tends to preserve cellular architecture better than with methanol, we first used a paraformaldehyde fixation protocol to investigate the effects of AlF_4^- on the cellular distribution of native RGS14. In untreated (control) cells, immunofluorescence and confocal imaging showed a relative enrichment of RGS14 around the nuclear membrane. Application of AlF_4^- lead to an increase in vesicle-like, punctate staining within the cytoplasm after 5 minutes and a significant decrease in nuclear membrane-to-cytoplasm fluorescence intensity by 10 minutes (**Figure 7a,b**). These data indicate that G protein activation by AlF_4^- causes a redistribution of RGS14 from basal state cellular compartments around the nuclear membrane to vesicular structures within the cytoplasm.

Paraformaldehyde fixation protocols tend to preserve cytoplasmic staining. Thus, due to the increase in cytosolic staining, fixation with paraformaldehyde could potentially mask staining of cytoskeleton-stabilized organelles, such as the endoplasmic reticulum and the Golgi. To correct for this, we performed the same AlF_4^--induced G protein activation protocol with methanol fixation. Similar to paraformaldehyde fixation, methanol fixation showed a decrease in RGS14 localization around the nuclear membrane, but also an accumulation of RGS14 in clustered perinuclear dot-like structures after 10 minutes of stimulation with AlF_4^-. Co-staining with antibody markers for the trans-Golgi network (TGN, anti-TGN38) and Golgi (anti-GM130) showed that though the perinuclear RGS14 staining consistently localized to the same region as the TGN and Golgi, We observed no significant overlap between RGS14 and our TGN or Golgi markers (**Figure 7c**). Though not tested, the clustered RGS14 staining in the center of TGN and

Golgi folds could also reflect an increase in localization at microtubule organizing centers or centrosomes. Notably, we found a considerable increase in RGS14 localization at the plasma membrane in several cells fixed with both methanol (**Figure 7d**) and paraformaldehyde (data not shown) after stimulation with AlF_4^- for 15 minutes. Other cells continued to show an accumulation of RSG14 in vesicle-like structures within the cytoplasm, suggesting that AlF_4^--induced translocation is a dynamic process and RGS14 localization at the plasma membrane could be transient. Nevertheless, these data indicate that global G protein activation with AlF_4^- affects the basal state cellular distribution of RGS14 in B35 cells.

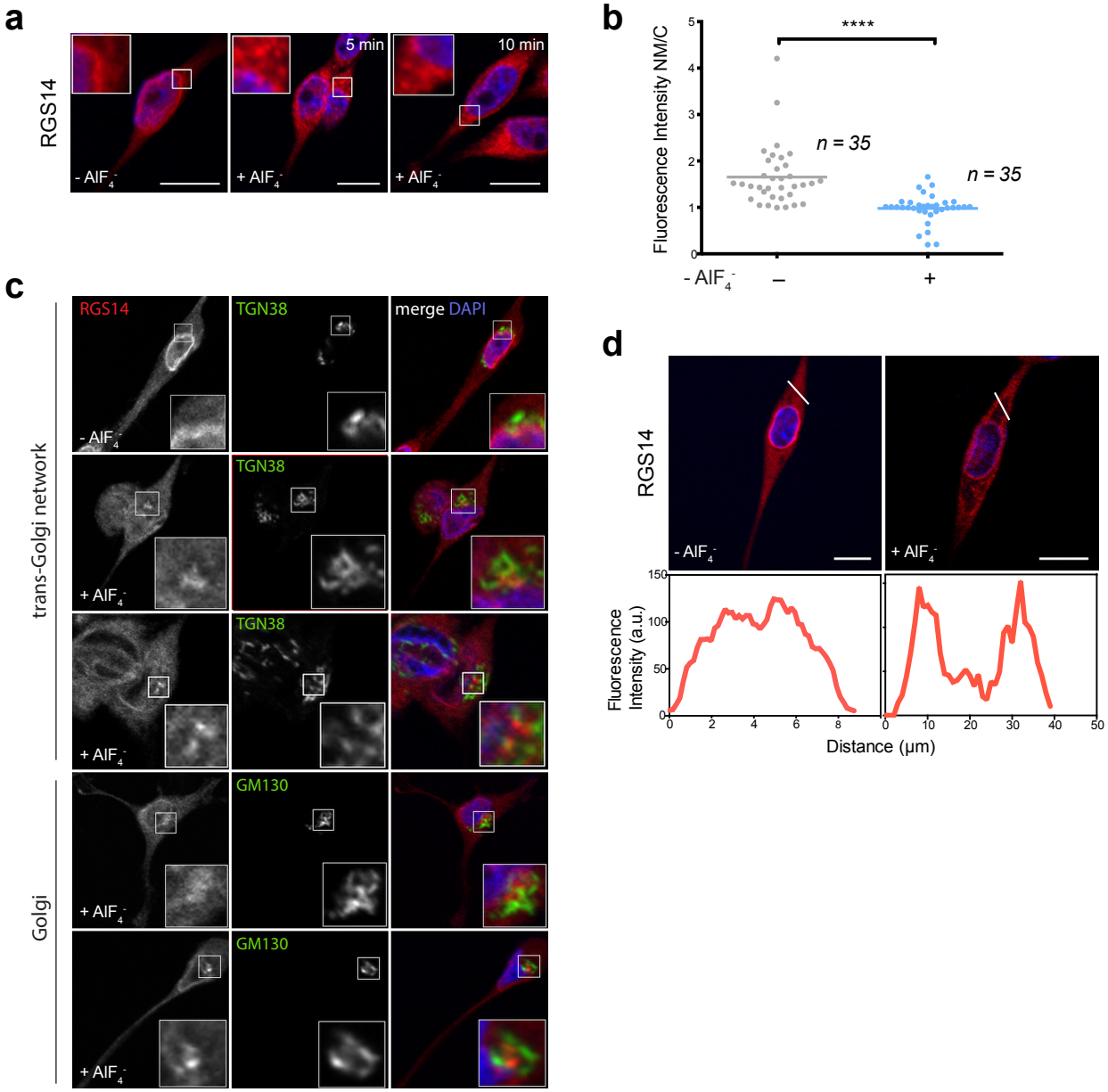
a
RGS14
5 min
10 min
- AlF4-
+ AlF4-
+ AlF4-
b
Fluorescence Intensity NM/C
****
n = 35
n = 35
- AlF4-
–
+
c
trans-Golgi network
Golgi
RGS14
TGN38
merge DAPI
GM130
d
RGS14
Fluorescence Intensity (a.u.)
Distance (μm)

Figure 7| G protein activation with AlF_4^- induces translocation of endogenous RGS14. Fluorescence microscopy analysis (**a**,**c**,**d**) and quantification (**b**) of endogenous RGS14 translocation from the nuclear membrane after G protein activation with AlF_4^-. A noticeable decrease in endogenous RGS14 localization around the nuclear membrane of B35 cells was observed 10 min after global G protein activation with AlF_4^-. (**a**) Confocal images of B35 cells incubated with or without (control) AlF_4^- for indicated times, fixed and permeabilized with paraformaldehyde/Triton-X and stained with an anti-RGS14 polyclonal antibody (pAb). (**b**) Scatterplot showing the ratio of nuclear membrane-to-cytosol localization of endogenous RGS14 in B35 cells fixed with paraformaldehyde following treatment with and without 10 min of AlF_4^- -induced G protein activation. Cells were fixed with 4% PFA in PHEM buffer and permeabilized with 0.1% Triton-X to prevent against possible cytoplasmic extraction during fixation/permeabilization with organic solvents (methanol and acetone). Enrichment of RGS14 at the nuclear membrane relative to cytosolic localization within B35 cells significantly decreased after treatment with AlF_4^- for 10 min (**a**,**c**). Nuclear membrane-to-cytosol localization of RGS14 was determined by dividing the average fluorescence intensity at the periphery of the nucleus (NM) by the average fluorescence intensity for a comparable area in the cytosol (C) (as depicted in **Supplementary Fig. 1**). Each point on the scatter plot represents the NM/C fluorescence intensity for a single cell immunostained with anti-RGS14 pAb and counterstained with Hoechst DNA dye (DAPI fluorescence channel) to locate nuclei (n = 35 cells for each experimental condition, 3 independent experiments). Horizontal line shows mean NM/C intensity ratio. ****P<0.0001 (Student t-test). Methanol fixation revealed an increase in localization of RGS14 within clusters around the trans-Golgi network (anti-TGN38) and Golgi (anti-GM130) after G protein activation with AlF_4^- for 10 min (**c**) and an observable increase in localization at the plasma membrane after 15 min (**d**).

We speculated that the apparent redistribution of endogenous RGS14 to the plasma membrane following treatment with AlF_4^- was due to binding of the RGS domain with AlF_4^- activated endogenous $G\alpha_{i/o}$ subunits residing on the plasma membrane. To determine whether exogenously expressed $G\alpha_{i/o}$ subunits affect the localization of endogenous RGS14, we initially transfected B35 cells with exogenous epitope-tagged $G\alpha_{i1}$-EE and $G\alpha_o$-EE cDNA. However, we found that immunofluorescence staining for endogenous RGS14 substantially decreased in B35 cells transfected with $G\alpha_i$ cDNA (**Supplementary Fig. 2**). The reason for this decrease in expression—observed only in the subpopulation of cells expressing $G\alpha_{i1}$—is currently unclear. Though speculative, overexpression of $G\alpha_{i1}$-GDP could lead to activation or inhibition of downstream signaling pathways that decrease RGS14 gene expression or increase degradation of the protein.

Thus, in order to investigate the effect of inactive $G\alpha_{i1}$ or $G\alpha_o$ on the cellular distribution of RGS14, we co-expressed exogenous FLAG-RGS14 with either $G\alpha_{i1}$-EE or $G\alpha_o$-EE in HeLa cells. Though the RGS domain of RGS14 interacts with activated $G\alpha_i$ and $G\alpha_o$ subunits, RGS14

also interacts with inactive $G\alpha_{i1}$-GDP through the GPR motif. Thus, we used $G\alpha_o$ to investigate whether the RGS domain plays a role in directing the subcellular localization of RGS14 in response to activation of $G\alpha_{i/o}$. For this investigation, HeLa cells were used instead of B35 cells due to a combination of good transfection efficiency, relatively large soma, and flat morphology ideal for examining plasma membrane localization. Exogenously expressed FLAG-RGS14 was predominantly localized diffusely throughout the cytoplasm in all cell lines tested (**Supplementary Fig. 3).** Co-expression of EE-epitope tagged $G\alpha_{i1}$ (Gαi1-EE-GDP) in HeLa cells was sufficient to recruit RGS14 to the plasma membrane. In contrast, FLAG-RGS14 remained in the cytosol when co-expressed with $G\alpha_o$-EE (**Fig. 8b**). Following G protein activation with AlF_4^-, FLAG-RGS14 remained at the plasma membrane with activated $G\alpha_{i1}$-EE. FLAG-RGS14 colocalized with activated $G\alpha_o$-EE at the plasma membrane after 10 min of treatment with AlF_4^- (**Fig. 8c**). Since RGS14 translocation to the plasma membrane by Gαo-AlF_4^- took place slowly over 10 minutes (**Fig. 8e**), it remains unclear whether RGS14 redistribution to the plasma membrane in response to signaling events downstream G protein activation or direct interactions with AlF_4^- activated $G\alpha_{i/o}$ through its RGS domain. Future investigations using a functional RGS14 mutant that does not bind activated $G\alpha_{i/o}$ subunits will be required to distinguish between these two possibilities. Nevertheless, the increased colocalization of FLAG-RGS14 and $G\alpha_o$-EE at the plasma membrane after treatment with AlF_4^-, suggests that once localized to plasma membrane, RGS14 interacts with activated $G\alpha_{i/o}$ subunits.

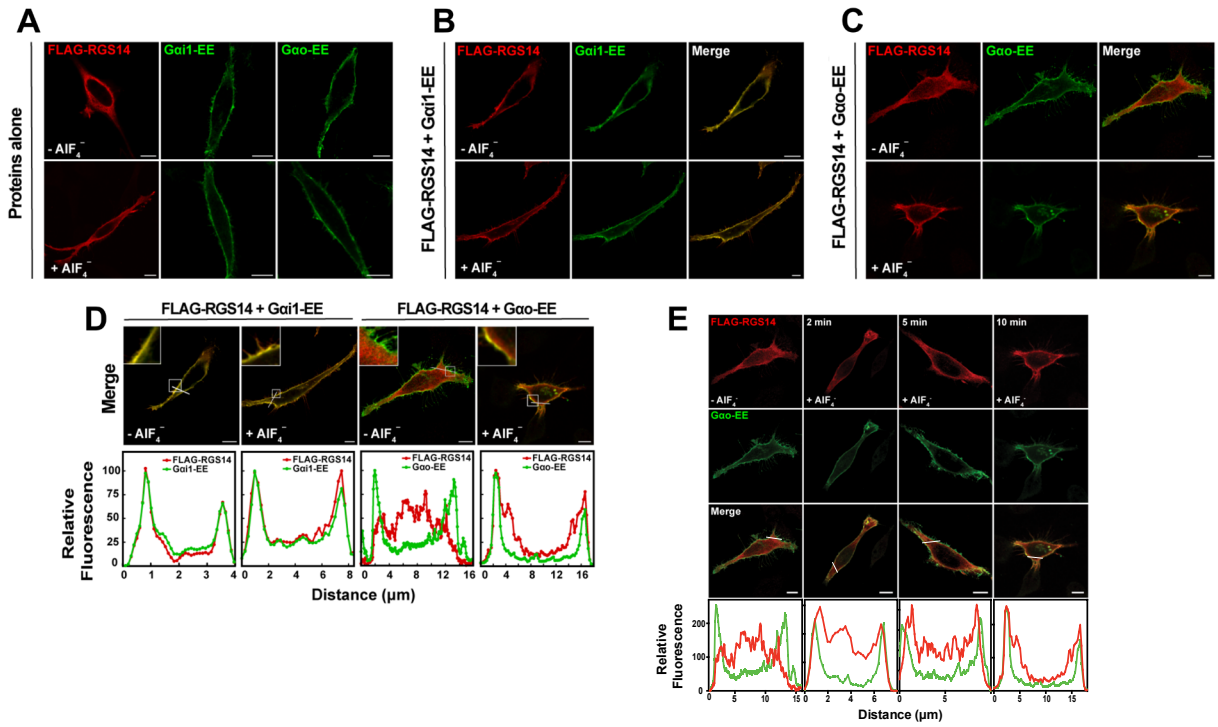

Figure 8| RGS14 is recurited to the pasma membrane in the presence of inactive Gαi1-EE AlF4- activated Gαo-EE. (A) HeLa cells were transfected with either 100ng FLAG-RGS14 or 100ng of EE-tagged Gα proteins. Transfected cells were treated with aluminum tertrafluoride (AlF4-) for 10 minutes prior to fixation. Images are representative of three separate experiments. (B) HeLa cells were co-transfected with 100 ng FLAG-RGS14 and 100 ng Gαi1-EE. Cells were treated with AlF4- and fixed as in (A). Images are representative of three independent experiments. (B) HeLa cells were co-transfected with 100 ng FLAG-RGS14 and 100 ng Gαo-EE. Cells were treated with AlF4- and fixed as in (A). Images are representative of three separate experiments. (D) Intensity graphs indicating relative fluorescence from merged images in (B) and (C). Relative fluorescence intensity of FLAG-RGS14 and either Gαi1-EE or Gαo-EE was measured at the plasma membrane as indicated by the white line in merged images. Intensity graphs were generated in ImageJ and are plotted from left to right along the indicated line. Insets highlight the plasma membrane in each image. Scale bar, 10 μm. (Brown et al., 2015)

This figure was originally published in The Journal of Biological Chemistry. Brown, N. E., Goswami, D., Branch, M. R., Ramineni, S., Ortlund, E. A., Griffin, P. R., & Hepler, J. R. (2015). Integration of G Protein Alpha (Gα) Signaling by the Regulator of G Protein Signaling 14. Journal of Biological Chemistry, jbc-M114. © the American Society for Biochemistry and Molecular Biology."

DISCUSSION

In the present study, we found that RGS14 exists in multiple populations within the cytoplasm and nucleus in B35 cells. Similar to previous reports about the localizations of exogenous RGS14 in other cell lines, endogenous RGS14 distributed to various compartments within the cytoplasm and localized to unidentified nuclear bodies. We found that the localization of endogenous RGS14 in nuclear bodies and perinuclear compartments in the vicinity of centrosomes was cell cycle-regulated. In addition and in contrast to reports describing the localization of exogenous RGS14, using an anti-RGS14 polyclonal antibody, we also detected prominent staining around the periphery of the nucleus that we have interpreted to be an association with the outer or inner nuclear membrane and a potential localization on the surface of mitochondria. Though further experiments, such as RNA interference-mediated knockdown and subcellular fractionation, are needed to confirm the specificity of the antibodies and localization of endogenous RGS14 in B35 cells, this is the first study to demonstrate a possible role for RGS14 at the nuclear membrane and on or within mitochondria. Furthermore, we showed that treatment of cells with AlF_4^- leads to a relocalization of endogenous and exogenous RGS14, suggesting that G protein activation is another mechanism capable of affecting the spatiotemporal profile of RGS14 in cells. Taken together, these findings provide further support to the idea that RGS14 is a multifunctional protein that is dynamically regulated to serve many roles in its native cellular environment.

Table 2. Subcellular localization of endogenous RGS14 in B35 cells

Subcellular localization of endogenous RGS14 in B35 cells (using pAb)	**Cellular state**
Cytosol	Basal
Nucleus	Basal
Nuclear bodies	Basal—potentially cell cycle-dependent
Nuclear membrane	Basal
Mitochondria	Basal
Vicinity of centrosomes	Cell cycle-dependent
Midzone	Anaphase/telophase
Midbody	Cytokinesis
Microtubules	At the midbody during cytokinesis

RGS14 in cell division

Our findings suggest that the localization of endogenous RGS14 near centrosomes—possibly within the surrounding pericentriolar material—is likely cell cycle-dependent in B35 cells. We also found that RGS14 colocalizes with α-tubulin at the midbody during cytokinesis. These results are consistent with previous reports showing a cell cycle-dependent association of exogenous RGS14 with centrosomes and localization at the midbody during cytokinesis in HeLa cells (Cho et al., 2004; Cho et al., 2007; Shu et al., 2007). While the functions of RGS14 at the midbody are currently unclear, various RGS14 binding partners, including Rap2 and novel interacting partner 14-3-3, exhibit similar midbody localization during cytokinesis—supporting the notion that RGS14 acts as a nexus for integrating various signaling events (Mukai et al., 2008; Du et al., 2011; Telkoparan et al., 2013, Gerber et al., 2015).

RGS14 and the cytoskeleton

Various studies have implicated heterotrimeric G proteins in regulating microtubule dynamics (Roychowdhury et al., 1999; Willard and Crouch., 2000; Roychowdhury et al., 2006; Dave et al., 2009). RGS14 has also been implicated in regulating microtubule stability and binds to polymerized, but not depolymerized, tubulin *in vitro* and in cells, likely through interactions with $G_{\alpha i/o}$ (Martin-McCaffrey et al., 2005). In B35 cells, methanol fixation revealed that AlF_4^--induced G protein activation caused endogenous RGS14 to translocate from the nuclear membrane to unidentified cytoplasmic bodies surrounded by trans-Golgi network and Golgi folds (**Fig. 7c**). In animal cells during interphase, the Golgi and centrosome share a close spatial relationship in a compact region on one side of the nucleus (Kupfer et al., 1983) along what is considered the nuclear-centrosomal axis. The nuclear-centrosomal axis is thought to be important for microtubule-based vesicular trafficking and organization, nuclear positioning, and maintenance and/or generation of cell polarity (reviewed in Luxton and Gunderson, 2011). Though not investigated in this study, it is possible that these unidentified nuclear bodies are associated with the centrosome or microtubule organizing center. In B35 cells, AlF_4^--induced G protein activation could cause RGS14 to translocate to the centrosome through direct interactions with activated $G\alpha_{i/o}$ subunits. This is an intriguing possibility considering that exogenous RGS14 and a constitutively active mutant of $G\alpha_{i1}$ were found to colocalize with centrosome marker γ-tubulin when co-expressed in HeLa cells (Shu et al., 2007). At centrosomes, RGS14 and $G\alpha_{i/o}$ may work together to modulate microtubule dynamics. Alternatively, RGS14 translocation to centrosomes may be intermediate to its transport to the plasma membrane along microtubules or via Golgi-derived recycling endosomes (**Fig. 10**).

In differentiated, non-dividing neurons, microtubules are critical for long-distance transport between the soma and distal dendrites and axons. Though the reorganization of the actin-cytoskeleton within post-synaptic spines as essential to the formation and maintenance of mature synapses is well established (Hotulainen and Hoogenraad, 2010) there has been recent evidence to suggest that microtubule dynamics also serve a critical role in structural synaptic plasticity. Dynamic microtubules have been shown to grow into dendritic spines in response to neuronal activity, calcium influx, and interactions with the actin-cytoskeleton (Merriam et al., 2013). The frequency of microtubule spine invasion correlates with the degree of activity-dependent spine enlargement (Jaworski et al., 2009). The growth of microtubules into dendritic spines may provide additional structural support during and after synapse formation and challenges the original belief that microtubule-dependent cargo transport is restricted to dendritic shafts (Kennedy and Ehlers, 2006). Based on the known involvement of RGS14 and $G_{\alpha i}$ in modulating microtubule dynamics, it is, thus, reasonable to postulate that interactions between RGS14, $G_{\alpha i}$ and microtubules are critical to RGS14-mediated LTP suppression in CA2 pyramidal neurons (**Fig. 11**). Consistent with this idea, co-immunoprecipitation of RGS14 from mouse brain coupled with mass spectrometry identified many cytoskeleton proteins—including myosin-14 and several microtubule associated proteins (MAPs)—as potential RGS14 interacting partners in neurons. Further additional studies will be required to determine whether RGS14 limits LTP by restricting functional or structural plasticity, or both.

RGS14 at the nuclear membrane

We observed that RGS14 had a similar, but non-overlapping, staining distribution around the periphery of the nucleus as the nuclear pore complex marker 414 mAb. Because the nuclear pore complex spans both the inner and outer nuclear membrane, higher resolution super

microscopy and/or co-staining with an antibody against an antigen localized exclusively to the inner or outer nuclear membrane will be needed to determine whether RGS14 is localized to the inner or outer nuclear membrane. Since the outer nuclear envelope is contiguous with the endoplasmic reticulum, it is possible that endogenous RGS14 is synthesized in the ER membrane from which it diffuses to the outer nuclear membrane where it interacts with cytoskeletal elements, such as microtubules. Positioned at the outer nuclear membrane, RGS14 could be involved in modulating nuclear positioning and cell polarity or could be dynamically transported through nuclear pores into the nuclear matrix, where it serves a currently unknown function (**Fig 10**).

RGS14 in the nucleus

Early reports on the subcellular localization of RGS14 in HeLa cells, found that GFP-tagged RGS14 predominantly localized to the cytoplasm and, in some cells, to perinuclear dot structures under basal conditions (Cho et al., 2005; Shu et al., 2007). In addition, these early investigations found that GFP-RGS14 accumulated in the nucleus after application of the nuclear export inhibitor leptomycin B and localized to subnuclear compartments following mild heat shock-induced cellular stress (Cho et al., 2005; Shu et al., 2007). These findings suggest that exogenously expressed recombinant RGS14 is a nucleocytoplasmic protein that rapidly shuttles into and out of the nucleus to serve diverse cellular roles, though its specific nuclear functions are still unclear. Using two different RGS14 antibodies, we found that endogenous RGS14 localized to unidentified nuclear compartments in B35 cells. The observed nuclear localization of endogenous RGS14 in B35 cells is unsurprising given that RGS14 contains at least three putative nuclear localization signals (NLS) and a nuclear export signal (NES) (**Fig. 9**).

The punctate distribution of RGS14 within the nucleus was found within most cells under basal conditions, but appeared to be most pronounced in cells in late S/early G2 phases (determined by the observation of duplicated/paired centrosomes)(**Fig. 6a**), indicating a possible cell cycle-dependence. The nucleus contains many highly organized compartments with unique functions. These nuclear bodies (NBs) serve diverse roles in various activities within the nucleus, including pre-mRNA synthesis and processing, mRNA and protein trafficking between the nucleus and cytoplasm and between the various nuclear compartments, and DNA repair (reviewed in Zimber et al., 2004). Among the most well-studied are promyelocytic leukemia (PML) and Cajal nuclear bodies (NBs). While Cajal NBs serve as the site of nuclear RNA biogenesis, PML NBs are implicated in the regulation of a wide variety of functions, including identification of foreign proteins and protein storage, post-translational modifications of proteins, transcriptional regulation, and chromatin organization (reviewed in Bernardi and Pandolfi, 2007). While some PML bodies are relatively static within the nucleus, others undergo highly dynamic changes in distribution and size both under basal conditions, throughout the cell cycle, and in response to cellular stress, such as heat shock and DNA damage. Though, in this study, we did not attempt to identify which specific nuclear compartments native RGS14 localizes to within B35 cells, exogenous RGS14 has been reported to translocate to PML bodies in HeLa cells following heat shock (Cho et al., 2005).

The PML protein is a tumor suppressor necessary for the formation of PML NBs (Fu et al., 2005). PML protein undergoes post-translational modification by covalent attachment of a small ubiquitin-like modifier (SUMO) and SUMOylation is required for the localization of many proteins to PML NBs (Zhong et al., 2000). Using a SUMOylation sequence analysis database (http://www.abgent.com/sumoplot), we identified two putative high consensus SUMOylation motifs (SUMO) and one inverted SUMOylation consensus motif (iSUMO, defined as

[ED]xK[VILFP])(Matic et al., 2010) on RGS14 (**Fig. 9**). The presence of several SUMOylation sites within the amino acid sequence of RGS14 supports the notion that native RGS14 localizes to PML NBs within B35 cells. Future investigation is needed, however, to determine whether RGS14 is SUMOylated *in vivo* and, if so, the effect of SUMOylation on its function and subcellular localization.

Recent studies have shown that several proteins involved in synaptic plasticity are SUMOylated (Martin et al., 2007). Moreover, SUMOylation is important for various neuronal processes including synapse formation and cell survival (reviewed in Henley et al., 2014), and global SUMO conjugation levels increase in response to neuronal activation (Lee et al., 2014). Though the role of global SUMOylation in regulating the synaptic stability of CA2 pyramidal is currently unknown, SUMOylation and/or translocation to the nucleus may be required for RGS14 to suppress LTP in CA2 pyramidal neurons. Additionally, if, like several other SUMOylated proteins found within NBs, RGS14 serves to regulate the transport of mRNA and/or RNA binding proteins, it is also possible that RGS14 serves a similar role in neurons by regulating the transport of large RNA riboneucleotide complexes between the nucleus and synapse to control local protein translation—which is critical to LTP (Bagni and Greenough, 2008; Berndt et al., 2012) (**Fig. 11**).

a

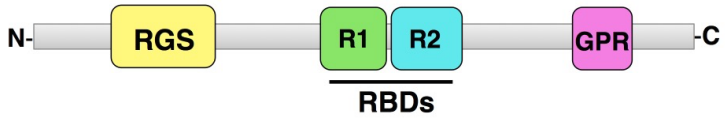

b

```
HUMAN         MPGKPKHLGV PNGRMVLAVS DGELSSTTGP QGQGEGRGSS LSIHSLPSGP SSPFPTEEQP        60
RAT           MPGKPKHLGV PNGRMVLAVS DGELTSTSGS QAQGEGRGSS LSIHSLPSGP SSPFSTDEQP        60
MOUSE         MPGKPKHLGV PNGRMVLAVS DGELTSTAGS QAQGEGRGSS LSIHSLPSGP SSPFSTEEQP        60
              ********** ********** ****:**:*  *.******** ********** **** *:***

                                      SUMO1
HUMAN         VASWALSFER LLQDPLGLAY FTEFLKKEFS AENVTFWKAC ERFQQIPASD TQQLAQEARN        120
RAT           VASWAQSFER LLQDPRGLAY FTEFLKKEFS AENVTFWQAC ERFQQIPASD TKQLAQEAHN        120
MOUSE         VASWAQSFER LLQDPRGLAY FTEFLKKEFS AENVTFWKAC ERFQQIPASD TKQLAQEAHN        120
              ***** **** ***** **** ********** *******:** ********** *:******:*

                                                                SUMO2
HUMAN         IYQEFLSSQA LSPVNIDRQA WLGEEVLAEP RPDMFRAQQL QIFNLMKFDS YARFVKSPLY        180
RAT           IYHEFLSSQA LSPVNIDRQA WLSEEVLAQP RPDMFRAQQL QIFNLMKFDS YARFVKSPLY        180
MOUSE         IYHEFLSSQA LSPVNIDRQA WLSEEVLAQP RPDMFRAQQL QIFNLMKFDS YARFVKSPLY        180
              **:******* ********** **.*****:* ********** ********** **********

                                      NLS1 (0.6)
HUMAN         RECLLAEAEG RPLREPGSSR LGSPDATRKK PKLKPGKSLP LGVEELGQLP PVEGPGGRPL        240
RAT           QECLLAEAEG RPLREPGSSH LGSPDTARKK PKLKPGKSLP LGVEELGQLP LAE---GRPL        237
MOUSE         QECLLAEAEG RPLREPGSSH LGSPDTARKK PKLKPGKSLP LGVEELGQLP LAEGPCGRPL        240
              :********* *********: *****::*** ********** **********  .*   ****
               NLS2  (0.3)
HUMAN         RKSFRREL-G GTANAALRRE SQGSLNSSAS LDLGFLAFVS SKSESHRKSL GSTEGESESR        299
RAT           RKSFRREMPG GAVNSALRRE SQGSLNSSAS LDLGFLAFVS SKSESHRKSL GSGEGESESR        297
MOUSE         RKSFRREMTG GAMNSALRRE SQGSLNSSAS LDLGFLAFVS SKSESHRKSL GSGESESESR        300
              *******: * *: *:***** ********** ********** ********** ** *.*****

                                                          SUMOi
HUMAN         PGKYCCVYLP DGTASLALAR PGLTIRDMLA GICEKRGLSL PDIKVYLVGN EQ-ALVLDQD        358
RAT           PGKYCCVYLP DGTASLALAR PGLTIRDMLA GICEKRGLSL PDIKVYLVGK EQKALVLDQD        357
MOUSE         PGKYCCVYLP DGTASLALAR PGLTIRDMLA GICEKRGLSL PDIKVYLVGN EQKALVLDQD        360
              ********** ********** ********** ********** *********: ** *******

                                      NLS3 (0.06)
HUMAN         CTVLADQEVR LENRITFELE LTALERVVRI SAKPTKRLQE ALQPILEKHG LSPLEVVLHR        418
RAT           CTVLADQEVR LENRITFQLE LVGLERVVRI SAKPTKRLQE ALQPILAKHG LSLDQVVLHR        417
MOUSE         CTVLADQEVR LENRITFQLE LVGLERVVRI SAKPTKRLQE ALQPILAKHG LSLDQVVLHR        420
              ********** *******:** *..******* ********** ****** *** **  :*****

HUMAN         PGEKQPLDLG KLVSSVAAQR LVLDTLPGVK ISKARDKSPC RSQGCPPRTQ DKATHPPPAS        478
RAT           PGEKQLVDLE NLVSSVASQT LVLDTLPDAK TREASSIPPC RSQGCLPRTQ TKDSHLPPLS        477
MOUSE         PGEKQPMDLE NPVSSVASQT LVLDTPPDAK MSEARSISPC RSQGCLPRTQ TKDSHLPPSS        480
              ***** :**  : *****:*  ***** * .*   :* .  ** ***** ****  * :* ** *

                                      NES
HUMAN         PSSLVKVPSS ATGKRQTCDI EGLVELLNRV QSSGAHDQRG LLRKEDLVLP EFLQLPAQGP        538
RAT           SSLSVEDASG STGKRQTCDI EGLVELLNRV QSSGAHDQRG LLRKEDLVLP EFLQLPSQRP        537
MOUSE         SSLLVEDASS STGNRQTCDI EGLVELLNRV QSSGAHDQRG LLRKEDLVLP EFLQLPSQRP        540
               *  *:  *. :**:****** ********** ********** ********** ******:* *

HUMAN         SSEETPPQTK SAAQPIGGSL NSTTDSAL        566
RAT           GSQEAPP--- ---------- --------        544
MOUSE         GSREAPP--- ---------- --------        547
              .*.*:**
```

Figure 9| Amino acid sequence of RGS14 predicts conserved NLS, NES, and SUMOylation motifs. (a) Cartoon of full-length RGS14 an its four binding domains. (b) Amino acid sequences of human, rat, and mouse RGS14. Amino acids corresponding to the RGS, R1, and R2 domains are highlighted in yellow, green, and cyan (respectively). Amino acids corresponding to the GPR motif are highlighted in magenta. Analysis of the RGS14 amino acid sequence predicted three nuclear localization signals (NLS1, NLS2, NLS3), a nuclear export signal (NES), two high consensus SUMOylation motifs (SUMO1, SUMO2), and one inverted SUMOylation motif (SUMOi) (underlined amino acids). Critical amino acids for each motif are in bold. Prediction strengths for the NLS motifs are in parenthesis. Asterisks (*) show conserved amino acids between the human, rat, and mouse RGS14 sequences.

In addition, a role for RGS14 in regulating transcription has been speculated for over a decade (Cho et al., 2005); however, the direct evidence for RGS14 mediated-transcriptional regulation is lacking. While the function(s) of nuclear RGS14 remain unclear, our findings provide additional evidence that endogenous RGS14 has roles in regulating cellular activity within the nucleus. Though native RGS14 in CA2 neurons from fixed hippocampal slices has not been reported in the nucleus (Lee et al., 2010), nuclear localization of RGS14 in neurons could depend on specific signals, including synaptic stimulation or neuronal stress. One intriguing possibility is that, in CA2 neurons, excitatory synaptic stimulation triggers RGS14 to be transported by microtubule-motors from the synapse to the nucleus. In the nucleus, RGS14 may directly or indirectly serve as a transcriptional regulator, thereby, influencing long-lasting changes in gene expression and subsequent synapse formation (**Fig. 11**).

RGS14 in Mitochondria

The mitochondria marker used in our analysis, HSP60, is a chaperone protein primarily located within the mitochondrial matrix in mammalian cells (Reviewed in Yogev and Pines, 2011); the absence of distinct colocalization (indicated by an obvious yellow color in the merged image), may be due to the fact that RGS14 is distributed along the surface of mitochondria and is absent from the inner mitochondrial matrix. In addition, the fact that this apparent punctate staining along the surface of mitochondria was not evident when cells were fixed with organic solvents that have been known to extract or cause mislocalization of unanchored cytosolic proteins (Asai., 2008; Stadler et al., 2010; Schnell et al., 2012), provides further support for the mitochondrial surface-level localization of RGS14.

Interestingly, using subcellular fractionation and immunofluorescence, two recent studies showed that endogenous $G\alpha_{i1}$ localizes on the surface of mitochondria in HEK293T and HeLa cells (Lyssand and Bajjalieh, 2007; Zhang et al., 2010). Notably, in both of these reports, the visual distribution of $G\alpha_{i1}$ along mitochondria showed an uneven, punctate staining pattern, similar to the uneven distribution we observed between endogenous RGS14 and mitochondria marker HSP60. Though the role of $G\alpha_{i1}$ in relation to mitochondria is currently unknown, endogenous $G\alpha_{12}$ is also found along mitochondria and is thought to regulate mitochondria motility and morphology (Andreeva et al., 2008) and $G_{\beta 2}$ has been shown to regulate mitochondrial fusion (Zhang et al., 2010).

In addition, possible interactions between $G_{\alpha i1}$ and RGS14 in relation to microtubule and mitochondria dynamics may not be entirely separate. Though speculative, reported roles for RGS14 and $G\alpha_{i1}$ in regulating tubulin polymerization (Martin-McCaffrey et al., 2005; Roychowdhury and Rasenick, 2008) suggest that, in B35 cells, RGS14 could interact with $G_{\alpha i}$ to modulate tubulin-dependent mitochondria trafficking, anchorage, and/or fusion/fission initiation (Jourdain et al., 2009; Liu et al., 2009) (**Fig. 10**).

Mitochondria play a fundamental role in ATP (energy) production, calcium homeostasis, and cell survival. Proper trafficking of mitochondria to post-synaptic terminals provides energy for metabolically demanding processes in response to synaptic activity and prevents cytotoxicity through calcium buffering (reviewed in Khatri and Man, 2013). Mitochondria transport and dynamic functions, such as calcium uptake and activity-dependent increases in reactive oxygen species (ROS) production are essential for LTP (Knapp, 2002; Kim et al., 2011). Though still speculative, the findings from this study provide evidence that RGS14 may associate with mitochondria, and in doing so, could modulate mitochondria trafficking, myosin-dependent

docking, fission/fusion, or calcium-dependent ROS production to limit synaptic plasticity in CA2 pyramidal neurons (**Fig. 11**).

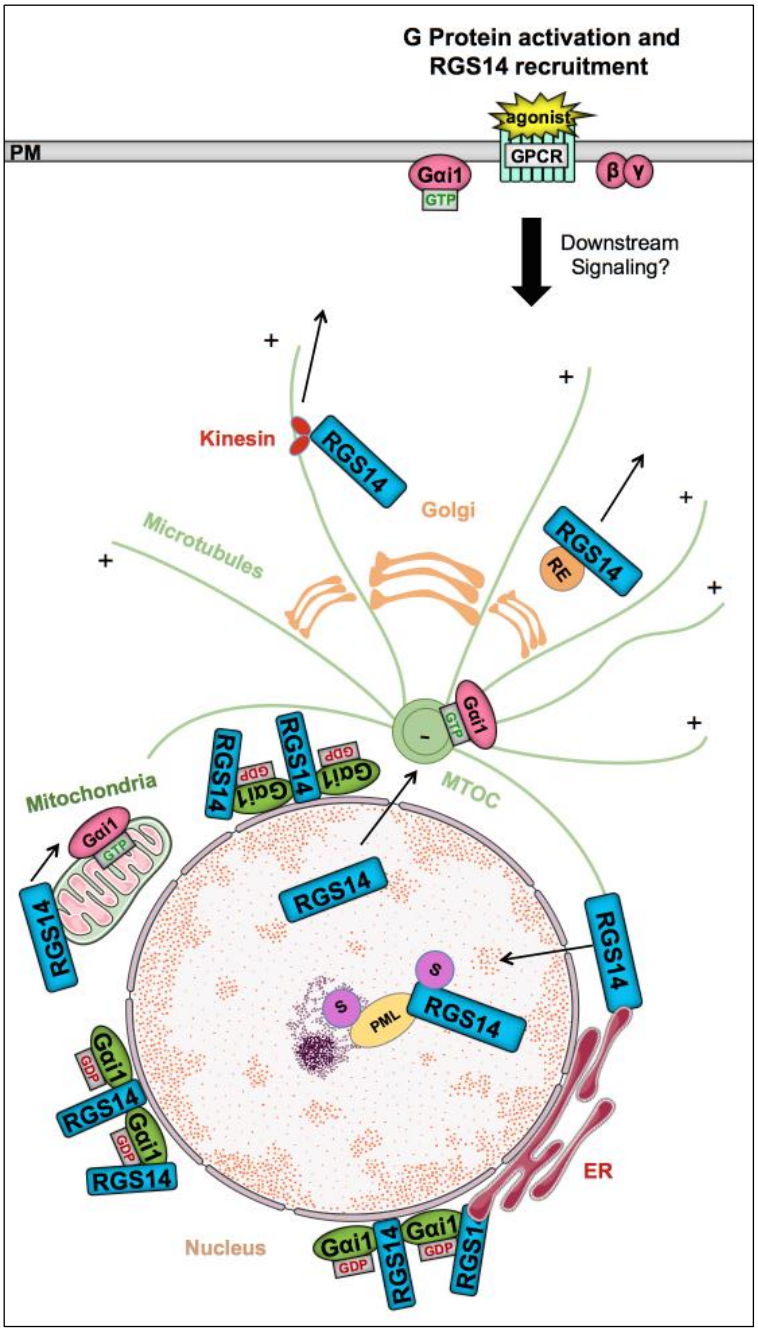

Figure 10 | Proposed model for the spatiotemporal regulation of endogenous RGS14 in B35 cells after G protein activation. In B35 cells, endogenous RGS14 is localized within the cytoplasm, around the nuclear membrane, on the surface of mitochondria, and in nuclear bodies under basal conditions. Nuclear localization and/or targeting to nuclear bodies (such as PML NBs) could be regulated by covalent attachment of SUMO to one of the putative SUMOylation consensus motifs on RGS14. Following AlF_4^--induced G protein activation, RGS14 could be directly recruited by activated Gα binding partners to microtubule organizing centers within centrosomes where it may modulate microtubule dynamics. Alternatively, AlF_4^-- induced centrosome localization could serve as an intermediate "stop" from which RGS14 could either be directly trafficked along microtubules by retrograde molecular motors (kinesin) to the plasma membrane or pass through endosomal compartments from which it is transported to the plasma membrane via recycling endosomes PM, plasma membrane; RE, recycling endosomes; MTOC; microtubule organizing center; PML, promyelocytic leukemia protein; S, post-translational modification by SUMO.

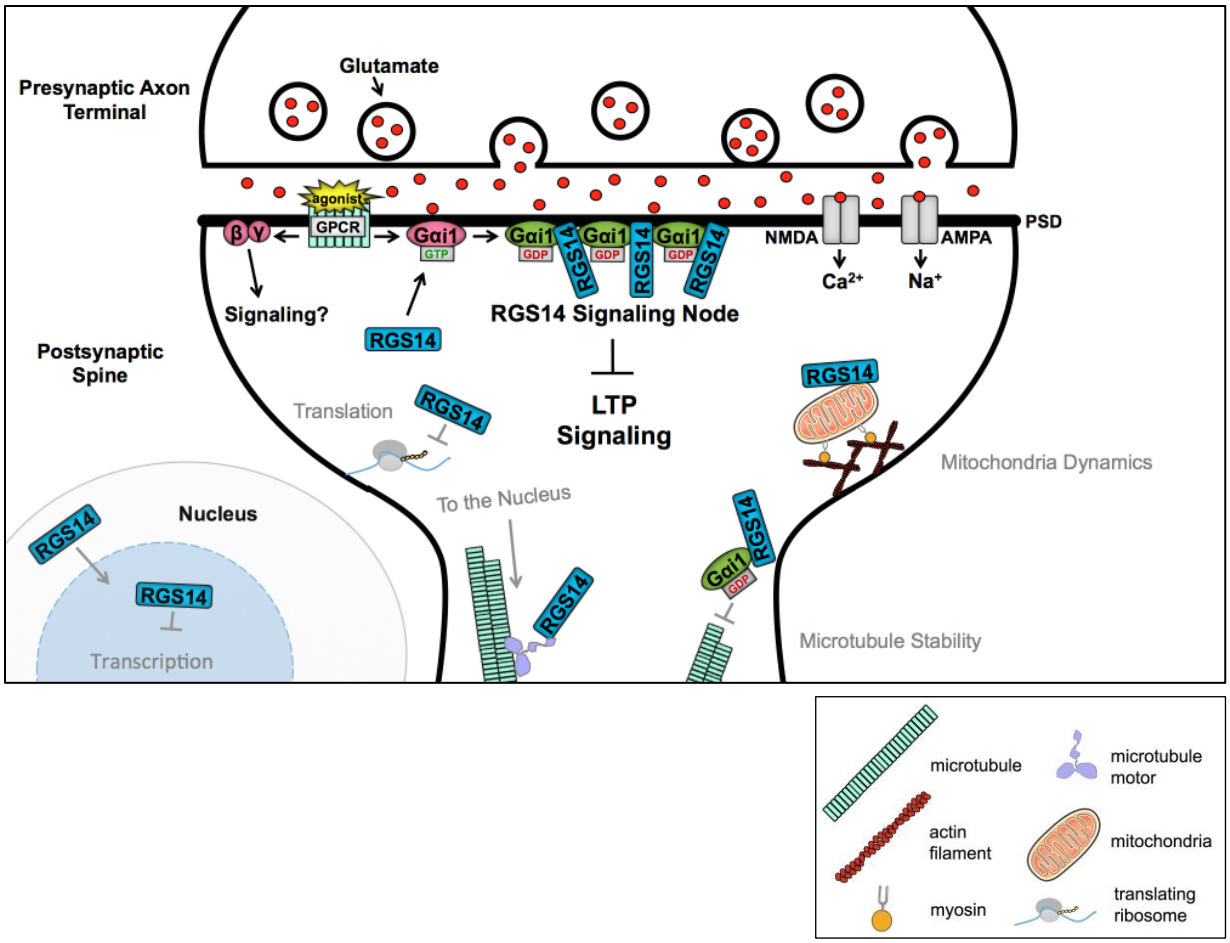

Figure 11| Schematic illustrating possible mechanisms by which RGS14 limits synaptic plasticity in CA2 hippocampal neurons. In CA2 neurons, activated $G\alpha_{i/o}$-GTP subunits could recruit RGS14 to post-synaptic spines following coincident activation ionotropic glutamate receptors (NMDA and AMPA) and a G protein coupled receptor (GPCR). After inactivating $G\alpha_{i/o}$-GTP subunits by stimulating GTP hydrolysis, RGS14 may form a signaling complex with inactive $G\alpha_{i/o}$-GDP subunits at the post-synaptic density (PSD). Membrane bound RGS14·$G\alpha_{i1}$ complexes may then act in a signaling nexus to block incoming excitatory neurotransmission through interactions with various protein. Activity-dependent complexes between RGS14 and $G\alpha_{i1}$ could also affect synaptic plasticity by prolonging Gβγ downstream signaling pathways. (*Transcription*) In addition, RGS14 could also act as a transcriptional repressor. (*To the Nucleus*) Upon NMDA receptor activation, RGS14 may be retrogradely transported along microtubules by molecular motors, such as kinesin and dynein, from synapses to the nucleus where it acts in opposition to LTP-promoting transcriptional activators to limit synaptic plasticity. In this way, RGS14 may mediate both immediate LTP-induction and long-lasting changes in gene expression. (*Translation*) Since local translation at stimulated synapses is critical for LTP (reviewed in Bramham et al., 2007), RGS14 could serve as a transcript-specific translational repressor or modulate the transport and targeting of mRNA or translational machinery to distal synapses. (*Mitochondria Dynamics*) Mitochondria transport and dynamic functions, such as calcium uptake and activity-dependent increases in reactive oxygen species (ROS) production are essential for LTP (Knapp, 2002; Kim et al., 2011). Though still highly speculative, the findings from this study provide evidence that RGS14 may associate with mitochondria and in doing so could modulate mitochondria trafficking, myosin-dependent docking, fission/fusion, or calcium-dependent ROS production to suppress LTP. (*Microtubule Stability*) The extent of calcium and F-actin-dependent microtubule spine invasion correlates with synaptic activity (Merriam et al., 2013). Moreover, dynamic microtubules are important for synaptic plasticity and synapse maturation (Jaworski et al., 2009). It is, therefore, possible that RGS14 interacts with $G\alpha_{i1}$ to limit microtubule dynamics and prevent the formation of stable synapses (model adapted from Brown et al., 2015).

CONCLUSION

Based on the findings from this study and others, we propose possible mechanisms by which RGS14 localization in B35 cells is dynamically regulated by G protein activation (Fig. 10) and offer several hypothetical models by which RGS14 could act to limit synaptic plasticity in CA2 pyramidal neurons (**Fig. 11**). Our findings suggest that in B35 cells, endogenous RGS14 is localized within the cytoplasm, around the nuclear membrane, on the surface of mitochondria, and in nuclear bodies under basal conditions. Following AlF_4^--induced G protein activation, RGS14 could be directly recruited by activated Gα binding partners to microtubule organizing centers within centrosomes where it may modulate microtubule dynamics. Alternatively, AlF_4^--induced centrosome localization could serve as an intermediate "stop" from which RGS14 could either be directly trafficked along microtubules to the plasma membrane or passes through endosomal compartments (such as the Golgi) from which it is transported to the plasma membrane by recycling endosomes (**Fig. 10**). Whether RGS14 translocation to the plasma membrane depends on direct interactions with activated Gα binding partners with the RGS domain remains to be determined. Nevertheless, our data suggest that, once at the plasma membrane, RGS14 interacts with activated $G\alpha_{i/o}$ subunits to terminate G protein signaling.

The results from this study provide further evidence that RGS14 is a complex multifunctional protein that has a variety of cellular functions. In addition, our findings demonstrate that the spatiotemporal localization of RGS14 can be modulated by interactions with both inactive and activated Gα binding partners, and thus, depends on both its GPR motif and RGS domain (respectively). We also found that endogenous RGS14 in B35 cells localizes to many of the same subcellular compartments as exogenous RGS14 reported in previous studies, suggesting that exogenous and endogenous RGS14 have similar local properties. While our

ultimate goal is to understand the dynamic regulation and functions of endogenous RGS14 in CA2 neurons, isolation of CA2 neuronal cultures is currently unfeasible. The results from this study along with recent data showing that adenovirus (AAV)-mediated expression of RGS14 in CA1 hippocampal neurons is sufficient to suppress LTP (unpublished data), suggest, however, that a fluorescently-tagged RGS14 construct expressed in cultured CA1 neurons may serve as a reasonable alternative to investigating the spatiotemporal dynamics of native RGS14 in host CA2 neurons. Indeed, live cell imaging of fluorescently-tagged RGS14, will provide additional insight into the kinetic properties of RGS14 translocation in response to various stimulatory conditions. Moreover, our findings that G protein activation stimulates RGS14 to translocate to the plasma membrane motivate future areas of investigation to determine whether G protein activation through metabotropic glutamate receptors (mGluRs) regulates the subcellular localization of RGS14 in neurons and whether RGS14 also plays a role in modulating mGluR-dependent LTP. Toward the long-term goal of understanding the molecular mechanism(s) by which RGS14 limits synaptic plasticity in CA2 pyramidal neurons, our results showing that endogenous RGS14 localizes to multiple cellular compartments in host B35 cells and that both inactive and activated G proteins can regulate the spatiotemporal dynamics of RGS14 illustrate that RGS14 may have multiple and complex functions in CA2 neurons. Future studies will be aimed at determining which of these functions is critical for RGS14-mediated suppression of synaptic plasticity.

REFERENCES

Andreeva, A. V., Kutuzov, M. A., & Voyno-Yasenetskaya, T. A. (2008). Gα12 is targeted to the mitochondria and affects mitochondrial morphology and motility. *The FASEB Journal*, *22*(8), 2821-2831.

Archer, S., Millot, G., Daskalogianni, C., Scherl, A., Manoury, B., & Fåhraeus, R. (2013). Translation of pre-spliced RNAs in the nuclear compartment generates peptides for the MHC class I pathway. *Proceedings of the National Academy of Sciences*, 110(44), 17951-17956.

Asai, D. J., (2008). Immunofluorescence microscopy. *Current Protocols Essential Laboratory Techniques*, 9-2.

Bagni, C., & Greenough, W. T. (2005). From mRNP trafficking to spine dysmorphogenesis: the roots of fragile X syndrome. *Nature Reviews Neuroscience*, *6*(5), 376-387.

Benes, F. M., Kwok, E. W., Vincent, S. L., & Todtenkopf, M. S. (1998). A reduction of nonpyramidal cells in sector CA2 of schizophrenics and manic depressives. *Biological psychiatry*, *44*(2), 88-97.

Berman, D. M., Kozasa, T., and Gilman, A. G. (1996) The GTPase-activating protein RGS4 stabilizes the transition state for nucleotide hydrolysis. *The Journal of biological chemistry* 271, 27209-27212

Bernardi, R. and Pandolfi, P. P. (2007). Structure, dynamics and functions of promyelocytic leukaemia nuclear bodies. Nat. Rev. Mol. Cell Biol. 8, 1006-1016.

Berndt, A., Wilkinson, K. A., & Henley, J. M. (2012). Regulation of neuronal protein trafficking and translocation by SUMOylation.*Biomolecules*, *2*(2), 256-268.

Bramham, C. R., & Wells, D. G. (2007). Dendritic mRNA: transport, translation and function. *Nature Reviews Neuroscience*, 8(10), 776-789.

Brown, N. E., Goswami, D., Branch, M. R., Ramineni, S., Ortlund, E. A., Griffin, P. R., & Hepler, J. R. (2015). Integration of G Protein Alpha (Gα) Signaling by the Regulator of G Protein Signaling 14. *Journal of Biological Chemistry*, jbc-M114.

Caruana, D. A., Alexander, G. M., and Dudek, S. M. (2012). New insights into the regulation of synaptic plasticity from an unexpected place: Hippocampal area CA2. *Learning & Memory*, *19*(9), 391-400.

Cho, H., Kozasa, T., Takekoshi, K., De Gunzburg, J., & Kehrl, J. H. (2000). RGS14, a GTPase-activating protein for Giα, attenuates Giα-and G13α-mediated signaling pathways. *Molecular pharmacology*, *58*(3), 569-576.

Cho, H., Harrison, K., Schwartz, O., & Kehrl, J. (2003). The aorta and heart differentially express RGS (regulators of G-protein signalling) proteins that selectively regulate sphingosine 1-phosphate, angiotensin II and endothelin-1 signalling. *Biochem. J*, 371, 973-980.

Cho, H., Kim, D. U., & Kehrl, J. H. (2005). RGS14 is a centrosomal and nuclear cytoplasmic shuttling protein that traffics to promyelocytic leukemia nuclear bodies following heat shock. *Journal of Biological Chemistry*, 280(1), 805-814.

Cho, H., & Kehrl, J. H. (2007). Localization of Giα proteins in the centrosomes and at the midbody: implication for their role in cell division. *The Journal of cell biology*, 178(2), 245-255.

Dave, R. H., Saengsawang, W., Yu, J. Z., Donati, R., & Rasenick, M. M. (2009). Heterotrimeric G-proteins interact directly with cytoskeletal components to modify microtubule-dependent cellular processes. *Neuro-Signals*, 17(1), 100.

Du, J., Chen, L., Luo, X., Shen, Y., Dou, Z., Shen, J., ... & Yao, X. (2011). 14-3-3zeta cooperates with phosphorylated Plk1 and is required for correct cytokinesis. *Frontiers in bioscience (Scholar edition)*, *4*, 639-650.

Dulin NO, Sorokin A, Reed E, Elliott S, Kehrl JH, Dunn MJ.(1999). RGS3 inhibits G protein-mediated signaling via translocation to the membrane and binding to Gα11. Mol Cell Biol.;19:714–723.

Evans, P. R., and Hepler, J. R. (2012) Regulator of G protein Signaling 14 (RGS14) interacts with calmodulin (CaM) in a calcium-dependent manner. , Society for Neuroscience (Abstract) 44.04., New Orleans, Louisiana.

Evans, P. R., Lee, S. E., Smith, Y., and Hepler, J. R. (2014). Postnatal developmental expression of regulator of G protein signaling 14 (RGS14) in the mouse brain. *Journal of Comparative Neurology*, *522*(1), 186-203.

Fu, C., Ahmed, K., Ding, H., Ding, X., Lan, J., Yang, Z., ... & Yao, X. (2005). Stabilization of PML nuclear localization by conjugation and oligomerization of SUMO-3. *Oncogene*, 24(35), 5401-5413.

Gerber, K., Seyfried, N., & Hepler, J. R. (2015). Pharmacology - Heterotrimeric G Protein and Second Messenger Signaling: Regulator of G protein Signaling 14 (RGS14) Interacts with 14-3-3 via an H-Ras and Gαi-dependent Mechanism, *FASEB*, (29), 618.13

Henley, J. M., Craig, T. J., & Wilkinson, K. A. (2014). Neuronal SUMOylation: Mechanisms, Physiology, and Roles in Neuronal Dysfunction. *Physiological reviews*, *94*(4), 1249-1285.

Hitti, F.L. & Siegelbaum, S.A. (2014) The hippocampal CA2 region is essen- tial for social memory. *Nature*, 508, 88–92.

Hollinger, S., Taylor, J. B., Goldman, E. H., & Hepler, J. R. (2001). RGS14 is a bifunctional regulator of Gαi/o activity that exists in multiple populations in brain. *Journal of neurochemistry*, *79*(5), 941-949.

Hollinger S, Hepler JR. (2002) Cellular regulation of RGS proteins: modulators and integrators of G protein signaling. *Pharmacological reviews* 54(3):527-59

Hollinger S, Ramineni S, Hepler JR (2003) Phosphorylation of RGS14 by protein kinase A potentiates its activity toward G alpha i. *Biochemistry* 42:811–9.

Hotulainen, P., & Hoogenraad, C. C. (2010). Actin in dendritic spines: connecting dynamics to function. *The Journal of cell biology*,*189*(4), 619-629.

Jaworski, J., Kapitein, L. C., Gouveia, S. M., Dortland, B. R., Wulf, P. S., Grigoriev, I., ... & Hoogenraad, C. C. (2009). Dynamic microtubules regulate dendritic spine morphology and synaptic plasticity. *Neuron*, *61*(1), 85-100.

Jourdain, I., Gachet, Y., & Hyams, J. S. (2009). The dynamin related protein Dnm1 fragments mitochondria in a microtubule-dependent manner during the fission yeast cell cycle. *Cell motility and the cytoskeleton*, *66*(8), 509-523.

Kennedy, M. J., & Ehlers, M. D. (2006). Organelles and trafficking machinery for postsynaptic plasticity. *Annual review of neuroscience*, *29*, 325.

Khatri, N., & Man, H. Y. (2013). Synaptic activity and bioenergy homeostasis: implications in brain trauma and neurodegenerative diseases. *Frontiers in neurology*, *4*.

Kim, H. Y., Lee, K. Y., Lu, Y., Wang, J., Cui, L., Kim, S. J., ... & Chung, K. (2011). Mitochondrial Ca2+ uptake is essential for synaptic plasticity in pain. *The Journal of Neuroscience*, 31(36), 12982-12991.

Kimple, R. J., De Vries, L., Tronchere, H., Behe, C. I., Morris, R. A., Gist Farquhar, M., and Siderovski, D. P. (2001) RGS12 and RGS14 GoLoco motifs are G alpha(i) interaction sites with guanine nucleotide dissociation inhibitor Activity. *The Journal of biological chemistry* 276, 29275-29281

Kirino, T. (1982). Delayed neuronal death in the gerbil hippocampus following ischemia. *Brain* research, 239(1), 57-69.

Knapp, L. T., & Klann, E. (2002). Potentiation of hippocampal synaptic transmission by superoxide requires the oxidative activation of protein kinase C. *The Journal of neuroscience*, 22(3), 674-683.

Kupfer, A., Dennert, G., & Singer, S. J. (1983). Polarization of the Golgi apparatus and the microtubule-organizing center within cloned natural killer cells bound to their targets. *Proceedings of the National Academy of Sciences*, 80(23), 7224-7228.

Lee, S. E., Simons, S. B., Heldt, S. A., Zhao, M., Schroeder, J. P., Vellano, C. P., ... & Hepler, J. R. (2010). RGS14 is a natural suppressor of both synaptic plasticity in CA2 neurons and hippocampal-based learning and memory. *Proceedings of the National Academy of Sciences*, *107*(39), 16994-16998.

Lee, L., Dale, E., Staniszewski, A., Zhang, H., Saeed, F., Sakurai, M., ... & Arancio, O. (2014). Regulation of synaptic plasticity and cognition by SUMO in normal physiology and Alzheimer's disease. *Scientific reports*, *4*.

Lein, E. S., Callaway, E. M., Albright, T. D., & Gage, F. H. (2005). Redefining the boundaries of the hippocampal CA2 subfield in the mouse using gene expression and 3-dimensional reconstruction. *Journal of comparative neurology*, 485(1), 1-10.

Lipman, N. S., Jackson, L. R., Trudel, L. J., & Weis-Garcia, F. (2005). Monoclonal versus polyclonal antibodies: distinguishing characteristics, applications, and information resources. *ILAR journal*, 46(3), 258-268.

Liu, X., Weaver, D., Shirihai, O., & Hajnóczky, G. (2009). Mitochondrial 'kiss-and-run': interplay between mitochondrial motility and fusion–fission dynamics. *The EMBO Journal*, *28*(20), 3074-3089.

Luxton, G. G., & Gundersen, G. G. (2011). Orientation and function of the nuclear–centrosomal axis during cell migration. *Current opinion in cell biology*, 23(5), 579-588.

Lyssand, J. S., & Bajjalieh, S. M. (2007). The heretotrimeric G protein subunit Gαi is present on mitochondria. *FEBS letters*, *581*(30), 5765-5768.

Ma, H., & Poon, R. (2011). How protein kinases co-ordinate mitosis in animal cells. *Biochem. J*, 435, 17-31.

Martin, S., Wilkinson, K. A., Nishimune, A., & Henley, J. M. (2007). Emerging extranuclear roles of protein SUMOylation in neuronal function and dysfunction. *Nature Reviews Neuroscience*, *8*(12), 948-959.

Martin-McCaffrey, L., Willard, F. S., Pajak, A., Dagnino, L., Siderovski, D. P., & D'Souza, S. J. (2005). RGS14 is a microtubule-associated protein. *Cell Cycle*, *4*(7), 953-960.

Matic, I., Schimmel, J., Hendriks, I. A., van Santen, M. A., van de Rijke, F., van Dam, H., ... & Vertegaal, A. C. (2010). Site-specific identification of SUMO-2 targets in cells reveals an inverted SUMOylation motif and a hydrophobic cluster SUMOylation motif. *Molecular cell*, 39(4), 641-652.

Merriam, E. B., Millette, M., Lumbard, D. C., Saengsawang, W., Fothergill, T., Hu, X., ... & Dent, E. W. (2013). Synaptic regulation of microtubule dynamics in dendritic spines by calcium, F-actin, and drebrin. *The Journal of Neuroscience*, *33*(42), 16471-16482.

McCudden, C. R., Hains, M. D., Kimple, R. J., Siderovski, D. P., & Willard, F. S. (2005). G-protein signaling: back to the future. *Cellular and Molecular Life Sciences*, 62(5), 551-577.

Mittal, V., and Linder, M. E. (2004) The RGS14 GoLoco domain discriminates among Galphai isoforms. *The Journal of biological chemistry* 279, 46772-46778

Mukai, A., Mizuno, E., Kobayashi, K., Matsumoto, M., Nakayama, K. I., Kitamura, N., & Komada, M. (2008). Dynamic regulation of ubiquitylation and deubiquitylation at the central spindle during cytokinesis. *Journal of cell science*, *121*(8), 1325-1333.

Neves, G., Cooke, S. F., & Bliss, T. V. (2008). Synaptic plasticity, memory and the hippocampus: a neural network approach to causality. *Nature Reviews Neuroscience*, 9(1), 65-75.

North, A. J. (2006). Seeing is believing? A beginners' guide to practical pitfalls in image acquisition. *The Journal of cell biology*, 172(1), 9-18.

Oner S.S., Maher E.M., Breton B., Bouvier M. & Blumer JB. (2010) Receptor-regulated interaction of activator of G-protein signaling-4 and Galphai. *The Journal of biological chemistry*. 285(27):20588–20594.

Pagani, J.H., Zhao, M., Cui, Z., Williams Avram, S.K., Caruana, D.A., Dudek, S.M. & Young, W.S. (2014) Role of the vasopressin 1b receptor in rodent aggressive behavior and synaptic plasticity in hippocampal area CA2. *Mol*. *Psychiatry*., doi: 10.1038/mp.2014.47.

Roy AA, Lemberg KE, and Chidiac P (2003) Recruitment of RGS2 and RGS4 to the plasma membrane by G proteins and receptors reflects functional interactions. *Mol Pharmacol* **64:** 587–593.

Roychowdhury, S., Panda, D., Wilson, L., & Rasenick, M. M. (1999). G protein α subunits activate tubulin GTPase and modulate microtubule polymerization dynamics. *Journal of Biological Chemistry*, 274(19), 13485-13490.

Roychowdhury, S., Martinez, L., Salgado, L., Das, S., & Rasenick, M. M. (2006). G protein activation is prerequisite for functional coupling between Gα/Gβγ and tubulin/microtubules. *Biochemical and biophysical research communications,* 340(2), 441-448.

Sprang, S. R. (1997). G proteins, effectors and GAPs: structure and mechanism. *Current opinion in structural biology*, *7*(6), 849-856.

Schnell, U., Dijk, F., Sjollema, K. A., & Giepmans, B. N. (2012). Immunolabeling artifacts and the need for live-cell imaging. *Nature methods*, 9(2), 152-158.

Shu, F. J., Ramineni, S., Amyot, W., and Hepler, J. R. (2007) Selective interactions between Gi alpha1 and Gi alpha3 and the GoLoco/GPR domain of RGS14 influence its dynamic subcellular localization, *Cellular Signalling 19*, 163-176.

Sloviter, R. S. (1991). Permanently altered hippocampal structure, excitability, and inhibition after experimental status epilepticus in the rat: the "dormant basket cell" hypothesis and its possible relevance to temporal lobe epilepsy. *Hippocampus*, 1(1), 41-66.

Stadler, C., Skogs, M., Brismar, H., Uhlen, M. & Lundberg, E. (2010) A single fixation protocol for proteome-wide immunofluorescence localization studies. *J. Proteomics* 73, 1067–1078.

Stadler, C., Rexhepaj, E., Singan, V. R., Murphy, R. F., Pepperkok, R., Uhlén, M., ... & Lundberg, E. (2013). Immunofluorescence and fluorescent-protein tagging show high correlation for protein localization in mammalian cells. *Nature methods*, 10(4), 315-323.

Stevenson, E. L., & Caldwell, H. K. (2014). Lesions to the CA2 region of the hippocampus impair social memory in mice. *European Journal of Neuroscience*.

Telkoparan, P., Erkek, S., Yaman, E., Alotaibi, H., Bayık, D., & Tazebay, U. H. (2013). Coiled-Coil Domain Containing Protein 124 Is a Novel Centrosome and Midbody Protein That Interacts with the Ras-Guanine Nucleotide Exchange Factor 1B and Is Involved in Cytokinesis. *PloS one*, *8*(7), e69289.

Traver, S., Bidot, C., Spassky, N., Baltauss, T., De Tand, M. F., Thomas, J. L., Zalc, B., Janoueix-Lerosey, I., and Gunzburg, J. D. (2000) RGS14 is a novel Rap effector that preferentially regulates the GTPase activity of galphao. *The Biochemical journal* 350 Pt 1, 19-29

Vellano, C. P., Brown, N. E., Blumer, J. B., & Hepler, J. R. (2013). Assembly and Function of the Regulator of G protein Signaling 14 (RGS14)• H-Ras Signaling Complex in Live Cells Are Regulated by Gαi1 and Gαi-linked G Protein-coupled Receptors. Journal of Biological Chemistry, 288(5), 3620-3631.

Watson, N., Linder, M. E., Druey, K. M., Kehrl, J. H., and Blumer, K. J. (1996) RGS family members: GTPase-activating proteins for heterotrimeric G-protein alpha-subunits. *Nature* 383, 172-175.

Willard, F. S., & Crouch, M. F. (2000). Nuclear and cytoskeletal translocation and localization of heterotrimeric G-proteins. *Immunology and cell biology*, 78(4), 387-394.

Yogev, O., & Pines, O. (2011). Dual targeting of mitochondrial proteins: mechanism, regulation and function. *Biochimica et Biophysica Acta (BBA)-Biomembranes*, *1808*(3), 1012-1020.

Zhang, J., Liu, W., Liu, J., Xiao, W., Liu, L., Jiang, C., ... & Chen, Q. (2010). G-protein [beta] 2 subunit interacts with mitofusin 1 to regulate mitochondrial fusion. *Nature* communications, 1, 101.

Zhao M, Choi Y-S., Obrietan K., & Dudek S.M. (2007). Synaptic Plasticity (and the Lack Thereof) in Hippocampal CA2 Neurons. *The Journal of neuroscience*. 27(44):12025–12032

Zhong, S., Müller, S., Ronchetti, S., Freemont, P. S., Dejean, A., & Pandolfi, P. P. (2000). Role of SUMO-1–modified PML in nuclear body formation. *Blood*, *95*(9), 2748-2752.

Zimber, A., Nguyen, Q., Gespach, C. (2004). Nuclear bodies and compartments: functional roles and cellular signalling in health and disease, *Cellular Signalling*, 16(10), 1085-1104.

a

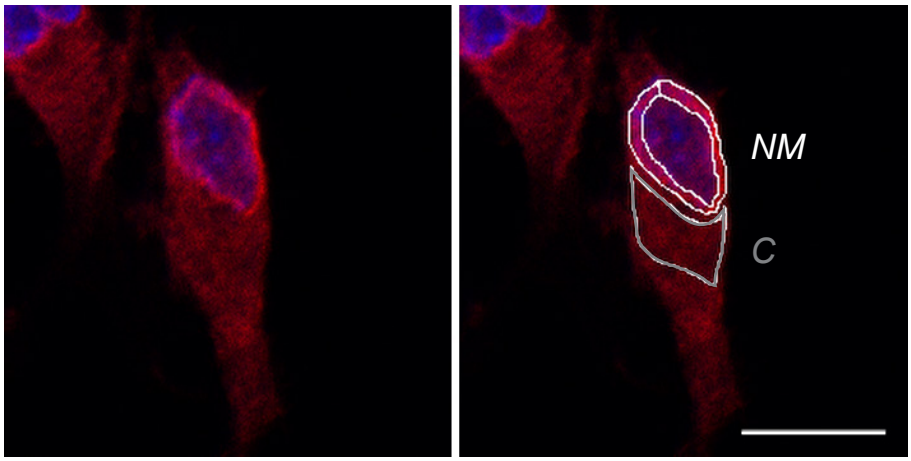

b

$$\text{Average Intensity} = \frac{\text{Total Fluorescence Intensity}}{\text{Area}}$$

$$\text{Fluorescence Intensity NM/C} = \frac{\text{Avg Intensity Nuclear Membrane}}{\text{Avg Intensity Cytosol}}$$

Supplementary Figure 1| Quantification of relative enrichment of RGS14 at the nuclear membrane following G protein activation with AlF4-. (a) Representative confocal image of an untreated (control) B35 cell fixed with paraformaldehyde and stained with the RGS14 polyclonal antibody (red) and counterstained with Hoechst DNA dye (left column). Right column shows the same cell with lines drawn around the nuclear membrane (white) and cytosol (gray) as described in Materials and Methods. Total fluorescence intensity was measured within the ring around the periphery of the nucleus (bounded by the white lines) and a comparable sized area within the cytosol (bounded by the gray lines) using ImageJ software. Scale bar, 10 μm. (b) Average fluorescence intensity was quantified by dividing the total fluorescence by the area of the measured region. The ratio of RGS14 nuclear membrane-to-cytosolic (NM/C) fluorescence intensity was determined by dividing the average fluorescence intensity at the nuclear membrane by the average fluorescence intensity within the cytosol (second equation).

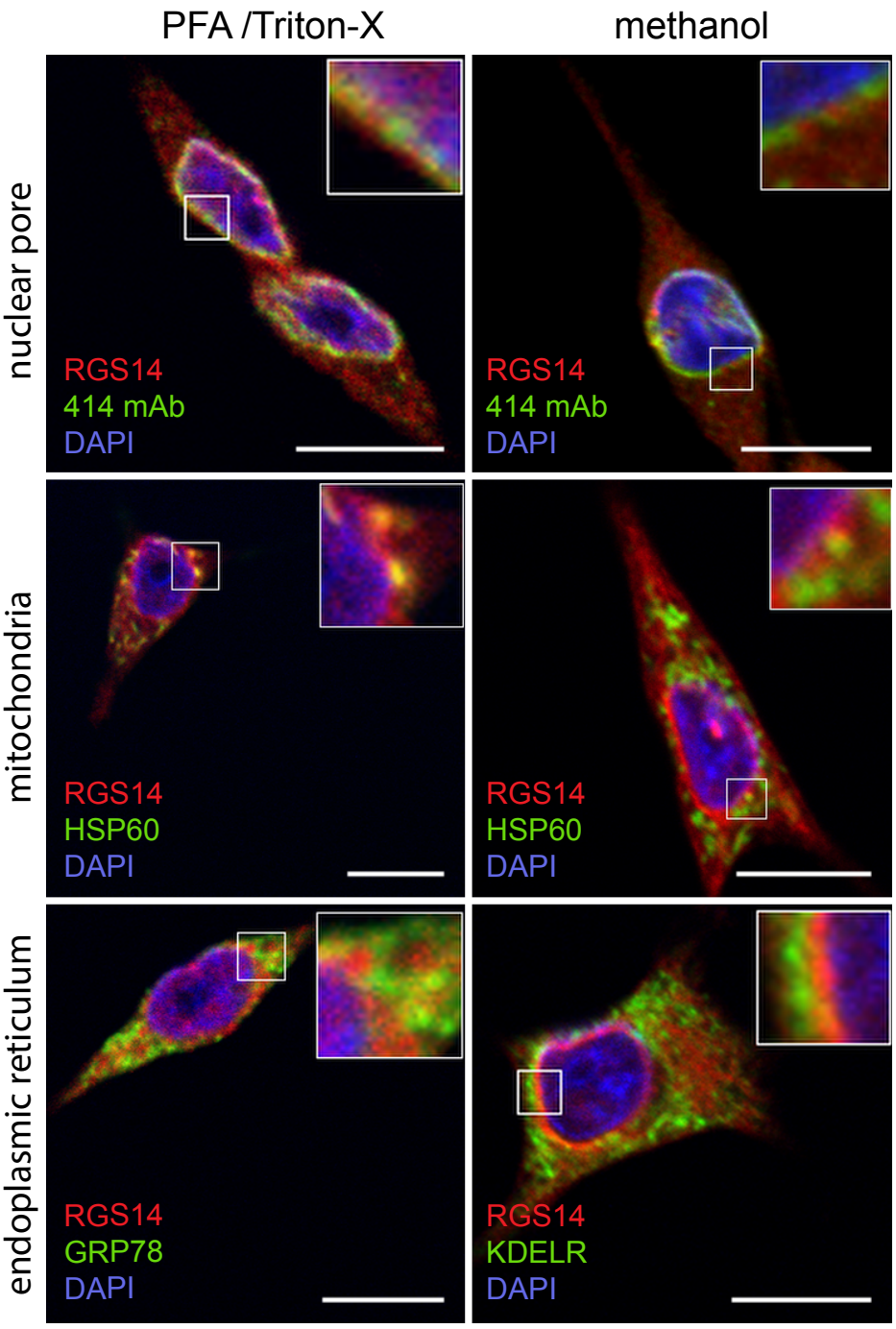

Supplementary Figure 2| Effect of paraformaldehyde and methanol fixation on RGS14 colocalization analysis. Confocal images of untreated B35 cells fixed with either 4% paraformaldehyde (PFA) for 10 min at room temperature and permeabilized with 0.1% Triton-X for 10 min (Column 1) or simultaneously fixed and permeabilized with ice cold methanol at -20 °C for 5 min (Column 2). Immunofluorescence was carried out as illustrated in the flow chart diagram in Fig. 1. B35 cells were co-stained with RGS14 polyclonal antibody (red) and an organelle marker (green)—414 mAb; nuclear pore complex; HSP60, mitochondria; GRP78 and KDELR, endoplasmic reticulum—and counterstained with Hoechst DNA dye (visualized under the DAPI channel). Insets represent magnified boxed regions. Scale bar, 10 μm.

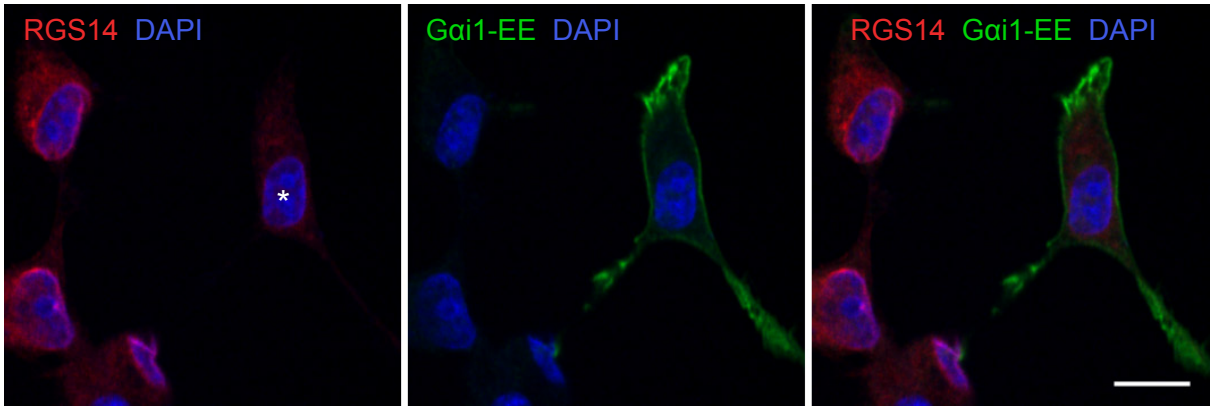

Supplementary Figure 3| Native RGS14 immunofluorescence intensity levels decrease in the presence of Gαi1-EE. Confocal image of B35 cells transfected with 500 ng of Gαi1-EE cDNA, co-stained with anti-RGS14 polyclonal antibody (red) and anti-EE (green), and counterstained with Hoechst DNA dye (visualized under the DAPI channel). The cell expressing visible levels of Gαi1-EE (*) shows substantially less RGS14 fluorescence signal compared with cells in which Gαi1-EE was not detected. Scale bar, 10 μm.

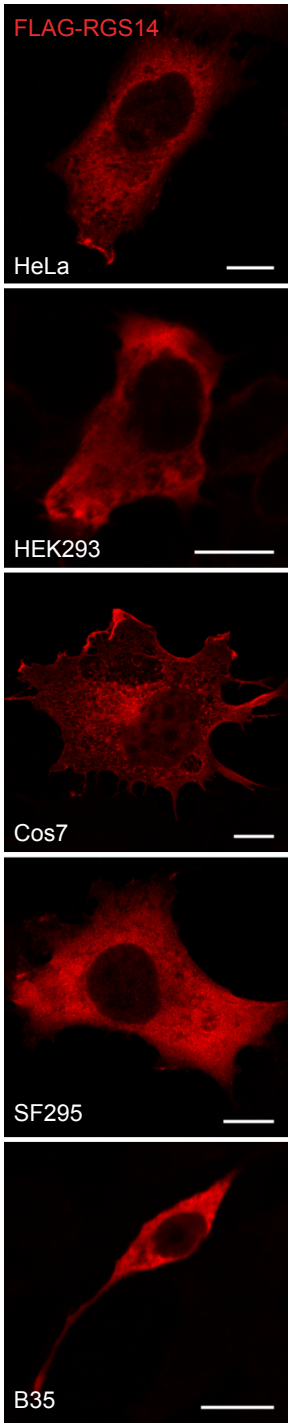

Supplementary Figure 4| FLAG-RGS14 is predominantly localized within the cytoplasm when expressed in various cell lines. HeLa, HEK293, Cos7, SF295, and B35 cells were transfected with 100-500 ng of FLAG-RGS14 cDNA. Cells were fixed with 4% paraformaldehyde in PBS, permeabilized with 0.1% Triton-X, and immunostained with an anti-FLAG antibody as described in Materials and Methods and as illustrated in flow chart diagram in Fig. 1.